Universitat
de les Illes Balears

DOCTORAL THESIS

2023

NEW HYBRID MATERIALS BASED ON METAL-ORGANIC FRAMEWORKS FOR THE REMOVAL OF ORGANIC POLLUTANTS

Neus Crespí Sánchez

Universitat de les Illes Balears

DOCTORAL THESIS

2023

Doctoral Programme in Chemical Science and Technology

NEW HYBRID MATERIALS BASED ON METAL-ORGANIC FRAMEWORKS FOR THE REMOVAL OF ORGANIC POLLUTANTS

Neus Crespí Sánchez

Thesis Supervisor: Gemma Turnes Palomino

Thesis Supervisor: Carlos Palomino Cabello

Thesis tutor: Gemma Turnes Palomino

Doctor by the Universitat de les Illes Balears

Universitat de les Illes Balears

Dra. Gemma Turnes Palomino and Dr. Carlos Palomino Cabello, of the Universitat de les Illes Balears

DECLARE:

That the thesis titled *New hybrid materials based on metal-organic frameworks for the removal of organic pollutants,* presented by Neus Crespí Sánchez to obtain a doctoral degree, has been completed under our supervision and meets the requirements to opt for an International Doctorate.

For all intents and purposes, we hereby sign this document.

Signatures

Dra. Gemma Turnes Palomino

Dr. Carlos Palomino Cabello

Palma de Mallorca, 16th of March, 2023

A mi familia

Agradecimientos

Después de muchos años de subidas y bajadas, dificultades múltiples, pero sobre todo muchísimo trabajo, por fin puedo decir que aquí termina este largo camino. Todo esto no habría sido posible sin la ayuda de tantas personas que directa o indirectamente me han guiado durante todo este trayecto.

En primer lugar, quiero agradecer a mis directores de tesis, el Dr. Carlos Palomino y la Dra. Gemma Turnes por haber confiado en mí, ya que, sin sus consejos, su ayuda y sobre todo su eterna paciencia no habría podido ir superando los distintos retos ni haber llegado hasta el final. GRACIAS por estar ahí en cada momento durante todos estos años.

Quiero dar las gracias también a los profesores de grupo de Química Ambiental de la UIB por toda la ayuda que me han prestado durante estos años, compartiendo quebraderos de cabeza con el HPLC y solucionando problemas técnicos.

Agradecer también a todos los técnicos del Servicio Técnico de la UIB por su ayuda a la hora de caracterizar todas las muestras descritas en este trabajo.

Al Ministerio de Educación y Ciencia por la concesión de una beca del Programa Nacional de Formación de Profesorado Universitario (FPU).

Quiero agradecer también al Ameloot Group de la KU Leuven por ayudarme y acogerme tan bien durante mi estancia, especialmente a Víctor por cada lección, y todo el apoyo, pero sobre todo para permitirme realizar la estancia bajo su supervisión

A todos mis compañeros de los grupos de Química de Materiales y Química Analítica ambiental que han compartido conmigo todo este trayecto. Especialmente a Marta y Mateu, empecé con vosotros esta loca aventura y no me habéis soltado de la mano en todo el camino, y a mis niñas Andrea y Virginia, por aparecer al final del camino y darme la energía necesaria para poder llegar al final. GRACIAS por las horas eternas de laboratorio, de charlas, confesiones, de bajones e infinitas risas. Sin vosotros nada de esto habría sido posible.

A todas las personas de las que he tenido suerte de rodearme en esta etapa. En especial a César, Edu, Enrique, Jesús, Sandy y Toni por ser luz, guiarme durante todo el camino y nunca dejarme rendir.

A todos mis amigos por apoyarme siempre y ayudarme a desconectar en los momentos más duros.

A mi familia, porque sin ellos no estaría hoy escribiendo estas líneas. Porque este trabajo es de vosotros. Gracias por todo el amor y apoyo, por enseñarme a no rendirme y ayudarme a superar los millones de obstáculos que han ido surgiendo. Por eso, este trabajo es por y para vosotros, porque GRACIAS a vosotros soy quien soy.

A todos vosotros, GRACIAS por compartir esta etapa de mi vida conmigo.

Abstract

The growing awareness of the negative effects that industrial and human activities have on the environment and public health and, more specifically, on water resources, has led to the development of new strategies to mitigate the impact of these activities and guarantee environmental quality standards, having become one of the most important social challenges today. Among the different strategies proposed to guarantee efficient water management, the development of materials that allow the extraction and elimination of environmental contaminants stands out as a key.

This Doctoral Thesis presents the development of new materials derived from metal-organic frameworks (MOFs) for the removal of organic contaminants such as dyes, phenols, and pharmaceutical products. As part of this process, different types of MOFs have been synthesized and used to the preparation of porous carbons and metal oxides. In order to facilitate their applicability, the prepared materials have been incorporated into supports such as membranes, magnetic stirrers and 3D printed devices. The obtained materials have been characterized with the adequate instrumental techniques and their applicability in the adsorption or photocatalytic degradation of different pollutants has been studied.

In the first work, the preparation of a carbon composite membrane derived from a MIL-125-NH_2 MOF has been carried out for the extraction of phenolic compounds. The derived carbon (C-MIL-125-NH_2) has been prepared by carbonization of the precursor MOF at a high temperature under nitrogen atmosphere. It has shown fast adsorption kinetics of bisphenol A and 4-tert-butylphenol, reaching equilibrium in 25 minutes. Moreover, with a simple coating process, a carbon composite membrane (C-MIL-125-NH_2-HM) has been obtained and tested in the dynamic extraction of the phenols under study, demonstrating good recyclability, excellent flow properties and a high efficiency for the preconcentration of both phenols.

In the second work, the preparation of a titanium oxide, derived from NTU-9 type metal-organic framework, has been described. This titanium oxide (TiO_2-NTU-9) was obtained by oxidation of the MOF precursor at 450 ^oC. TiO_2-NTU-9 has exhibited 100% of methylene blue (MB) degradation in 2 hours thanks to its mixed anatase/rutile phase structure, as well as carbon doping. In addition, by a simple deposition method, a mechanically stable TiO_2-NTU-9 coated stirrer (TiO_2-NTU-9-S) has been prepared and tested for the elimination of MB, demonstrating excellent and easy recyclability.

In the final work, to enhance the adsorption capacity of the MIL-100-Fe MOF, post-synthetic modification with sulfonic groups has been carried out by the grafting of aminomethanesulfonic acid (AMSA) onto the coordinatively unsaturated metal centers. The obtained, MIL-100-Fe-AMSA, has been used for the diclofenac (DCF) extraction, obtaining high extraction capacity (476 $mg \cdot g^{-1}$) thanks to the great affinity between DCF and the sulfonic groups. The functionalized MOF was immobilized in a 3D printing column, facilitating its use for the extraction, pre-concentration and analysis of low levels of DCF and ketoprofen in water samples.

Resum

La creixent sensibilització respecte als efectes negatius que les activitats industrials i humanes tenen sobre el medi ambient i la salut pública i, més concretament, sobre els recursos hídrics, ha donat lloc al desenvolupament de noves estratègies per a la mitigació de l'impacte que tenen aquestes activitats, convertint-lo en un dels reptes socials més importants en l'actualitat. Entre les estratègies proposades per garantir una gestió eficient de l'aigua i el compliment de les normes de qualitat ambiental, es troba el desenvolupament de materials que permetin l'extracció i l'eliminació de contaminants ambientals.

En la present Tesis Doctoral s'ha duit a terme el desenvolupament de nous materials derivats de xarxes metal·loorgàniques (MOFs) per a la eliminació de contaminants tals com colorants, fenols i productes farmacèutics. Per la qual cosa s'han sintetitzat diferent tipus de MOFs i, a partir d'aquests s'han preparat carbons porosos i òxids metàl·lics. A més, amb l'objectiu de facilitar la seva aplicabilitat, els materials preparats s'han incorporats en suports com membranes, agitadors magnètics o dispositius impresos en 3D. Els diferents materials obtinguts s'han caracteritzat mitjançant les tècniques instrumentals adequades i s'ha estudiat la seva aplicabilitat per a l'adsorció o degradació fotocatalítica de diferents contaminants.

En el primer treball s'ha duit a terme la preparació d'un membrana composta d'un carbó porós derivat d'una xarxa metal·loorgànica de tipus MIL-125-NH_2 per a l'extracció de composts fenòlics. El carbó derivat (C-MIL-125-NH_2) s'ha preparat mitjançant la carbonització a alta temperatura del MOF precursor en atmosfera de nitrogen. El material obtingut ha demostrat una ràpida cinètica d'adsorció de bisfenol A i 4-tert-butilfenol, assolint l'equilibri en 25 minuts. A més, amb un senzill procés de recobriment, s'ha obtingut una membrana composta d'aquest carbó (C-MIL-125-NH_2-HM) per a l'extracció en flux dels fenols en estudi, demostrant una bona reciclabilitat, excel·lent propietats de flux i una elevada eficiència per a la preconcentració de ambdós fenols.

En el segon treball s'ha descrit la preparació d'un òxid de titani derivat d'una xarxa metal·loorgànica de tipus NTU-9. Aquest òxid de titani (TiO_2-NTU-9) s'ha obtingut mitjançant l'oxidació a 450 ^oC del MOF precursor. El TiO_2-NTU-9 assoleix el 100% de degradació del blau de metilè (MB) en 2 hores gràcies a que presenta una estructura mixta de fase anatasa i rutil, així com un dopatge de carboni. A més, mitjançant un mètode de deposició simple, s'ha preparat un agitador recobert de l'òxid de titani (TiO_2-NTU-9-S) i s'ha aplicat a la eliminació de MB, demostrant una excel·lent i fàcil reciclabilitat.

Finalment, en el tercer i darrer treball, per tal de potenciar la capacitat d'adsorció de la xarxa metal·loorgànica MIL-100-Fe, s'ha duit a terme la modificació post-sintètica de la mateixa amb grups sulfònics mitjançant la incorporació del àcid aminometansulfònic (AMSA) en el centres metàl·lics descoordinats. El material obtingut, MIL-100-Fe-AMSA, s'ha utilitzat per a l'extracció de diclofenac (DCF), obtenint una elevada capacitat d'extracció (476 $mg \cdot g^{-1}$) gràcies a la gran afinitat del DCF per el grups sulfònics. El MOF funcionalitzat s'ha immobilitzat en una columna impresa en 3D, facilitant el seu ús per a l'extracció, preconcentració i anàlisis de baixos nivells de DCF i ketoprofén en mostres d'aigua.

Resumen

La creciente sensibilización respecto a los efectos negativos que las actividades industriales y humanas tienen sobre el medio ambiente y la salud pública y, más concretamente, sobre los recursos hídricos, ha dado lugar al desarrollo de nuevas estrategias para la mitigación del impacto que tienen estas actividades, convirtiéndolo en uno de los retos sociales más importantes en la actualidad. Entre las diferentes estrategias propuestas para garantizar una eficiente gestión del agua y el cumplimiento de las normas de calidad ambiental, se encuentra el desarrollo de materiales que permitan la extracción y eliminación de contaminantes ambientales.

En la presente Tesis Doctoral se ha llevado a cabo el desarrollo de nuevos materiales derivados de redes metalo-orgánicas (MOFs) para la eliminación de contaminantes orgánicos como colorantes, fenoles y productos farmacéuticos. Para ello, se han sintetizado diferentes tipos de redes metalo-orgánicas y a partir de estas se han obtenido carbones porosos y óxidos metálicos. Además, con el objetivo de facilitar su aplicabilidad, los materiales preparados se han incorporado en soportes como membranas, agitadores magnéticos o dispositivos impresos en 3D. Los diferentes materiales obtenidos han sido caracterizados con las técnicas instrumentales adecuadas y se ha estudiado su aplicabilidad en la adsorción o degradación fotocatalítica de diferentes contaminantes.

En el primer trabajo se ha llevado a cabo la preparación de una membrana compuesta de un carbón poroso derivado de una red metalo-orgánica tipo MIL-125-NH_2 para la extracción de compuestos fenólicos. El carbón derivado (C-MIL-125-NH_2) se ha preparado mediante la carbonización a elevada temperatura del MOF precursor en atmósfera de nitrógeno. El material obtenido ha demostrado una rápida cinética de adsorción del bisfenol A y el 4-tert-butilfenol, alcanzando el equilibrio en 25 minutos. Además, con un simple proceso de recubrimiento, se ha obtenido una membrana compuesta de este carbón (C-MIL-125-NH_2-HM) para la extracción en flujo de los fenoles en estudio, demostrando una buena reciclabilidad, excelentes propiedades de flujo y una elevada eficiencia para la preconcentración de ambos fenoles.

En el segundo trabajo se ha descrito la preparación de un óxido de titanio derivado de una red metalo-orgánica de tipo NTU-9. Este óxido de titanio (TiO_2-NTU-9) se ha obtenido mediante la oxidación a 450 ^oC del MOF precursor. El TiO_2-NTU-9 alcanza el 100% de degradación del azul de metileno (MB) en 2 horas gracias a que presenta una estructura mixta de fase anatasa y rutilo, así como un dopaje de carbono. Además, mediante un método de

deposición simple, se ha preparado un agitador magnético recubierto del óxido de titanio (TiO_2-NTU-9-S) y se ha aplicado en la eliminación de MB, demostrando una excelente y fácil reciclabilidad.

Finalmente, en el tercer y último trabajo, para potenciar la capacidad de adsorción de la red metalo-orgánica MIL-100-Fe, se ha llevado a cabo la modificación post-sintética de la misma con grupos sulfónicos mediante la incorporación del ácido aminometanosulfónico (AMSA) en los centros metálicos descoordinados. El material obtenido, MIL-100-Fe-AMSA, ha sido utilizado para la extracción de diclofenaco (DCF), obteniendo una elevada capacidad de extracción (476 $mg \cdot g^{-1}$), gracias a la gran afinidad del DCF por los grupos sulfónicos. El MOF funcionalizado se ha inmovilizado en una columna impresa en 3D, facilitando su uso para la extracción, preconcentración y análisis de bajos niveles de DCF y ketoprofeno en muestras de agua.

LIST OF PUBLICATIONS

This doctoral thesis is a compendium of the following research articles:

1. **Carbon composite membrane derived from MIL-125-NH_2 MOF for the enhanced extraction of emerging pollutants**

Authors**:** Neus Crespí Sánchez, Jorge Luis Guzmán-Mar, Laura Hinojosa-Reyes, Gemma Turnes Palomino y Carlos Palomino Cabello

Journal: Chemosphere

Year: 2019

Volume: 231

Pages: 510-517

DOI: 10.1016/j.chemosphere.2019.05.173

Impact factor: 5.778

2. **NTU-9 derived TiO_2 coated stirrer as a highly efficient device for photocatalysis**

Authors**:** Neus Crespí Sánchez, Gemma Turnes Palomino y Carlos Palomino Cabello

Journal: Materials Science and Engineering: B

Year: 2021

Volume: 273

Pages: 115424

DOI: 10.1016/j.mseb.2021.115424

Impact factor: 3.407

3. **Sulfonic-functionalized MIL-100-Fe MOF for the removal of diclofenac from water**

Authors**:** Neus Crespí Sánchez, Gemma Turnes Palomino y Carlos Palomino Cabello

Journal: Microporous and Mesoporous Materials

Year: 2023

Volume: 348

Pages: 112398

DOI: 10.1016/j.micromeso.2022.112398

Impact factor: 5.876 (2021)

Other publications derived from this thesis:

- Leo, P.; **Crespí, N.**; Palomino, C.; Martín, A.; Orcajo, G.; Calleja, G.; Martínez, F. (2021). Catalytic activity and stability of sulfonic-functionalized UiO-66 and MIL-101 materials in Friedel-Crafts acylation reaction. *Catal. Today*, *390-391*, 258-264.

- Martínez-Pérez-Cejuela, H.; Mompó-Roselló, Ó.; **Crespí-Sánchez, N.**; Palomino Cabello, C.; Catalá-Icardo, M.; Simó-Alfonso, E. F.; Herrero-Martínez, J.M. (2020). Determination of benzomercaptans in environmental complex samples by combining zeolitic imidazolate framework-8-based solid-phase extraction and high-performance liquid chromatography with UV detection. Journal of Chromatography A, 1631(461580), 461580.

INDEX OF CONTENTS

INDEX OF TABLES AND FIGURES

List of abbreviations

AMSA	Aminomethanesulfonic acid
BDDT	Brunauer-Deming-Deming-Teller
BET	Brunauer-Emmett-Teller
BPA	Bisphenol A
CUS	Coordinatively unsaturated sites
DCF	Diclofenac
DRS	Diffuse reflectance spectroscopy
EDAX	Energy dispersive X-ray analysis
Eg	Energy gap or band gap
FTIR	Fourier-transform infrared spectroscopy
H_3BTC	1,3,5-benzenetricarboxylic acid
HKUST	Hong Kong University of Science and Technology
HPLC	High performance liquid chromatography
MB	Methylene blue
MIL	Materials of Institute Lavoisier
MOF	Metal-organic framework
POPs	Persistent organic compounds
PVDF	Polyvinylidene fluoride
SEM	Scanning electron microscopy
TEM	Transmission electron microscopy
UiO	Universiteit i Oslo
UV-Vis	Ultraviolet-visible
ZIF	Zeolitic imidazolate framework
2D-NLDFT	Two-Dimensional Non-Local Density Functional Theory
4-tBP	4-tert-butylphenol

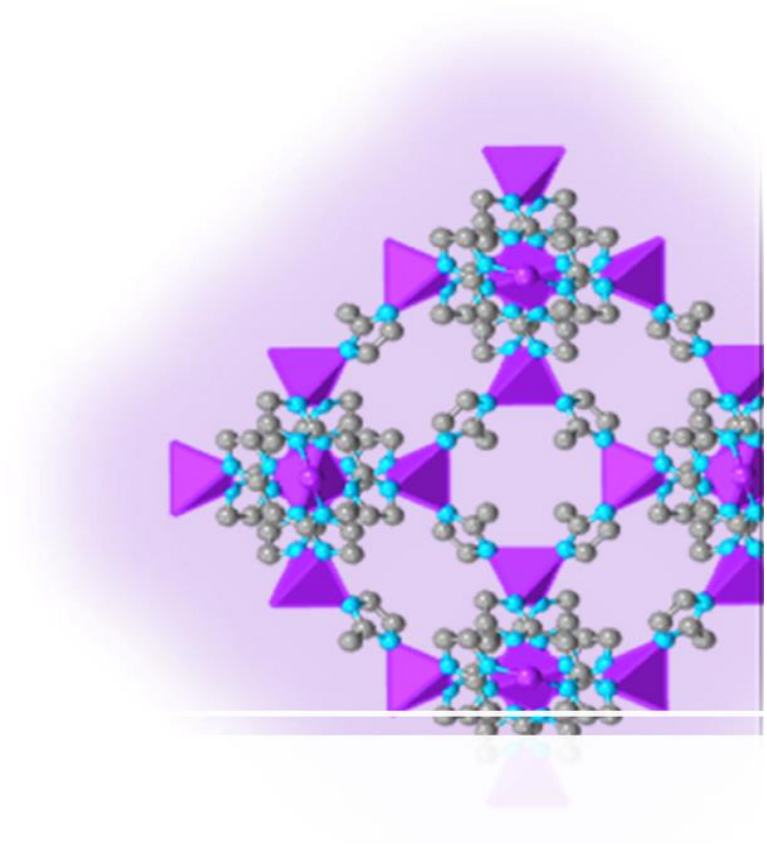

Chapter 1

Introduction

This chapter provides an extensive overview of metal-organic frameworks (MOFs). It includes a description of the properties of these novel materials and their potential applications. Chapter 1 also provides a detailed description of different types of materials derived from MOFs.

Chapter 1: Introduction

1.1. Overview of porous materials and their applications

Porous structures, such as molluscs or corals, have always been present in nature, and they played a fundamental role in the development of organisms. The first reported example of a porous material was activated carbon, discovered by the Egyptians.[1] Its porosity and high stability have made it a suitable adsorbent for the removal of colour, odour, taste, and other undesirable impurities and pollutants from drinking water[2,3] and air.[4,5]

Porous materials can be natural or synthetic, and the diversity of synthetic materials opens up the opportunity to develop different types of structures for specific purposes. Zeolites, which presents a crystalline three-dimensional aluminosilicate structure,[6] are one of the most important examples of this type of porous materials. Due to their natural abundance and the diversity of developed synthetic structures, they are widely applied in industrial processes such as air separation,[7,8] biogas or natural gas purification,[9,10] water disinfection,[11] drug delivery,[12] ion-exchange,[13] or in catalysis.[14]

The great number of industrial applications of both, activated carbons and zeolites, has motivated efforts to develop new porous materials, among which stand out mesoporous silicas, covalent organic frameworks (COFs), and metal-organic frameworks (MOFs).

1.2. Metal-organic frameworks (MOFs)

The discovery and development of metal-organic frameworks resulted from continuous research into the assembly of coordination polymers at the 1990s. The term MOF was introduced by Yagui et al., when they reported a diamond-like 3D structure formed by copper and 4,4'-bipyridine as a ligand.[15]

Metal-organic frameworks are porous crystalline solids based on the combination of metal centers or metal aggregates with multidentate organic ligands. This union results in the formation of open one-, two- or three-dimensional structures with an ordered system of pores (*Figure 1.1*).[16-18]

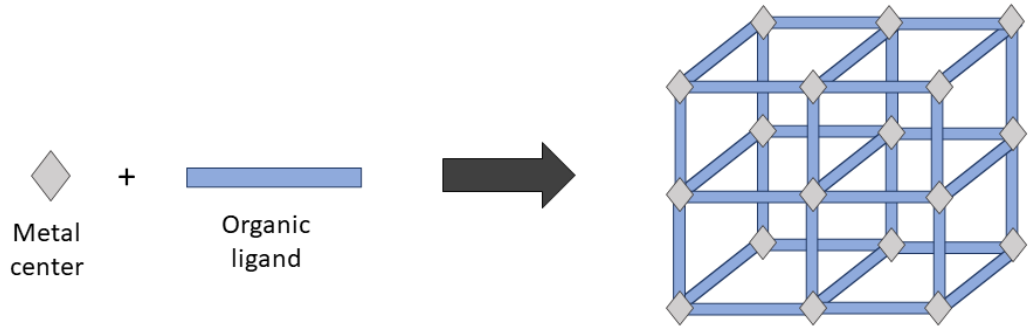

Figure 1.1. Formation of the structural skeleton of metal-organic frameworks.

Generally, the structure of porous materials, such mesoporous silicas or zeolites, is determined by molecular template or structural agent. In contrast, the porous cavities of MOFs are only determined by the geometric characteristics of their constituents.[19-21]

1.2.1. Properties

Metal-organic frameworks generally present an ordered porous system, formed by channels and cavities, with diameters ranging from 0.5 to 3.5 nm, which results in open structures with highly specific surface areas and pore volumes, with up to 80% of total volume being empty space. The pore sizes vary depending on the nature and length of the ligand molecules used, as well as the coordination chemistry of the metal centers.[22,23] The increment of the length of the ligands often causes the formation of interpenetrated metal-organic frameworks, in which two or more frameworks are physically interpenetrated, dividing the large pores into smaller ones (*Figure 1.2*).[24,25] The resulting framework generally has greater thermal and mechanical stability and, due to the formation of smaller cavities, its interaction with certain adsorbents can be increased, allowing the size discrimination of molecules.

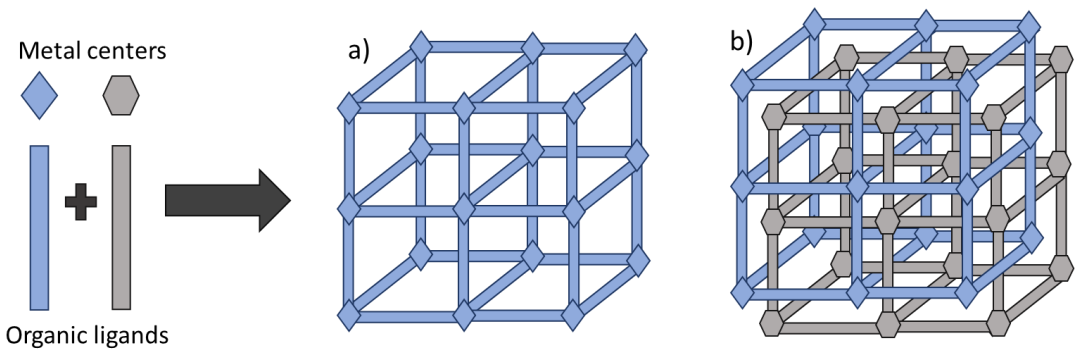

Figure 1.2. Schematic representation of the basic structure of: (a) non-interpenetrated and (b) interpenetrated framework.

The nature of MOFs metal centers is very diverse, being transition metal elements the most abundant.[26,27] However, in recent years, alkaline and alkaline earth metals, such as lithium or magnesium, have been used for the preparation of MOFs due to their potential application as lightweight materials for hydrogen storage.[28] There are also MOFs composed of lanthanides and actinides, as a consequence of their optical properties,[29] as well as elements from p-block.[30] In some MOFs, such as MOF-74 and MIL-100, the metal sites may be coordinated by one or more molecules of solvents, which, through a suitable heat treatment, can be removed, giving rise to the formation of coordinatively unsaturated sites (CUS) (*Figure 1.3*). The presence of these sites can be beneficial from the application point of view, as they can interact with host molecules, such as reagents or adsorbents.[31,32]

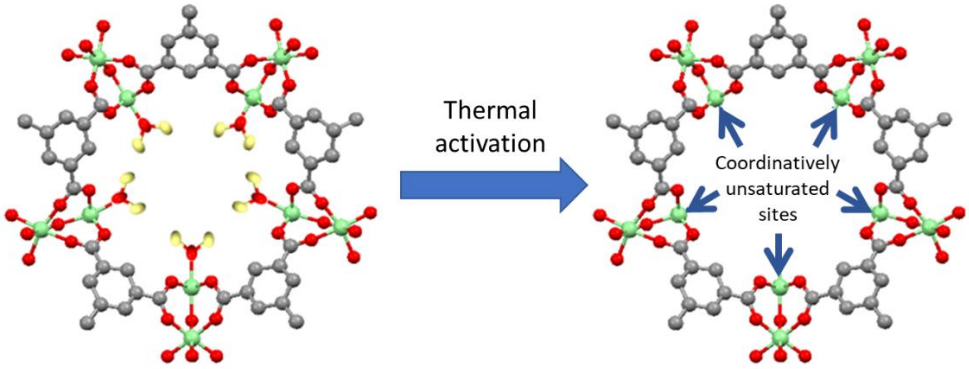

Figure 1.3. Schematic representation of the process for obtaining coordinatively unsaturated sites in MOFs.

In the case of linkers, different types of organic molecules have been used to join the metal centers. The first examples of MOFs were synthesized by the coordination of metal ions with oxygen atoms, coming mainly from ligands with carboxylate groups.[33,34] Since then, it has also been reported the preparation of MOF with nitrogenous linkers, such as pyrazole[35] or tetrazole.[36] As a result of the large number of available linkers and the different possible combinations with the various metal centers for the synthesis of MOFs, a huge number of different structures have been reported (*Table 1.1*).

Table 1.1. Different examples of most commonly used MOFs.

Metal center	Ligand	MOF
Zr	1,4-benzenedycarboxilate (BDC)	UiO-66
Cr, Fe	1,4-benzenedycarboxilate (BDC)	MIL-101
Zr	Byphenil-4,4'-dicarboxylate (BPDC)	UiO-67
Fe, Al, V, Cr	Benzene-1,3,5-tricarboxylate (H_3BTC)	MIL-100
Cu	Benzene-1,3,5-tricarboxylate (H_3BTC)	HKUST-1
Zn	2-methylimidazole (2-MIM)	ZIF-8
Co	2-methylimidazole (2-MIM)	ZIF-67
Zn	2-nitroimidazole (nIM)	ZIF-68
Cu, Mn, Fe, Zn	1,3,5-benzenetristetrazolate (BTT)	M-BTT
Cu, Mn, Fe, Mg, Co, Zn	2,5-dihydroxy-1,4-benzenedicarboxylate (DOBDC)	MOF-74

On the other hand, the possibility of modifying both, the organic ligands and the metal centers, by a post-synthetic procedure allows the obtention of MOFs with a wide variety of functional groups.[37,38] Examples include organic molecules, such as ethylenediamine,[39] doxorubicin[40] and polyethyleneimine,[41] and metals/metal clusters.[42,43] The functionalized MOFs can exhibit new and improved properties increasing their application in different fields, such as adsorption,[44-47] separation,[41,48] and catalysis.[42,49,50]

1.2.2. Applications

Owing to their unique advantages and versatility, MOFs have attracted increasing attention in recent years and have been extensively studied for applications in multiple fields. Gas storage is one of the most popular application of MOFs,[51-53] especially as hydrogen adsorbents for fuel storage,[54-56] with the aim of developing energy containers, as well as for carbon dioxide capture.[57]

MOFs have also shown enormous potential as heterogeneous catalysts due to the presence of different active sites in their structure.[58-60] They have proven to be efficient in various catalytic reactions such as the cyanosilation of aldehydes, the oxidation of alcohols, or the hydrogenation of olefins, as well as many other organic synthesis reactions.

Further applications include in the field of biomedicine, their use as a controlled drug release systems[61,62] or chemical sensors,[63] and, more recently, its application for the determination and removal of pollutants from water,[64-67] field in which MIL-101,[68] MIL-100[69] and UiO-66[70] MOFs stand out.

1.2.3. Synthesis of metal-organic frameworks

1.2.3.1. Solvothermal synthesis

Synthesis optimization in metal-organic frameworks is an essential step to obtain materials with desirable characteristics, mainly with regard to specific surface area, crystal size and morphology. Due to the wide variety of existing MOFs, a universal method for their preparation does not exist. In fact, different methods of synthesis have been developed to fulfil these needs. However, as a general rule, MOFs are prepared by the solvothermal method, which consists in the slow growth of crystals from a solution of organic and inorganic precursors at a given pressure, temperature and pH. A wide number of MOFs, such as HKUST-1,[71] and those of the ZIF[72], UiO[73,74] and MIL-100[75] families, have been synthesized for the first time using this method.

Many variables can influence the synthesis, the main ones to consider:

1. The temperature, which can range from room temperature to ~ 250 ^{o}C.

2. The pressure, self-generated inside the autoclave, depending on the temperature and the ratio volume of autoclave/volume of precursors solution.

3. The nature of the components, both the metal salt and the organic ligand, and their relative concentration.

4. The pH, which can vary over a wide range, depending on the MOF.

5. The reaction time, which can vary from hours to days.

6. The nature of the solvent used.

Because of the large number of parameters that influence the synthesis of MOFs, it is usually necessary to optimize the synthesis protocol. This optimization can be carried out using High-Throughput methods that allow studying the influence of different variables, having become a very useful tool for the development of new materials.[76]

Although the solvothermal method is the most used, it has some drawbacks, including the high reaction times and the difficulties of applying it on a large-scale synthesis. As a result, other synthesis procedures have been developed that imply shorter reaction times and less amounts of solvent.

1.2.3.2. Microwave synthesis

Microwave-assisted synthesis (MW synthesis) has been widely used for the preparation of different materials in inorganic chemistry.[77,78] Currently, this method is presented as one of the best alternatives to solvothermal synthesis since it can produce MOFs in very short times (minutes) and with greater control over the morphology and size of the crystals obtained.

MW synthesis is based on the interaction between electromagnetic waves with mobile electric charges, such as ions in solution and polar solvent molecules.[79] This interaction results in more efficient and faster heating, accelerating the nucleation stage and allowing the obtention of new crystalline phases. By using this method, the size of the crystals and their distribution are affected, being usually smaller and more homogeneous than those prepared by the solvothermal method.[80]

1.2.3.3. Electrochemical synthesis

Electrochemical synthesis represents a highly efficient method for the fabrication of nanostructured materials with advantages of low cost, low synthetic temperature, high purity, simplicity, and environmental friendliness.[81] In the synthesis of MOFs by this method, the metal cations diffuse to the reaction media through the anode and the organic linkers are dissolved into the electrolyte, where both react to each other. HKUST-1 electrochemical synthesis, in which a copper plate is immersed into a solution of H_3BTC linker, is one of the most common in the preparation of this material, allowing to obtain a MOF with a high surface area.[82]

1.2.3.4. Mechanochemical synthesis

Mechanochemical synthesis is a simple solid-state method based on a chemical reaction that occurs using the energy from the milling process. Among the advantages of the mechanochemical synthesis of MOFs are minimizing the cost of production by working at room temperature, decreasing in the use of solvents and reducing the number of process steps.[83,84]

However, it is important to mention that this method it cannot be considered solvent-free, since an additional-purification step is needed.

1.2.3.5. Sonochemical synthesis

In the sonochemical synthesis, the chemical reactions occur under an ultrasonic environment. The violent implosion of cavitation bubbles generates localized hot spots with exceedingly high transient temperatures (5000 K) and pressures (1800 atm), inducing crystal nucleation and growth.[85] However, the particle size is limited since those hot spots are characterized by extreme cooling rates, so the temperature of the reaction medium falls within milliseconds. By sonochemical method, and under mild synthetic conditions, different MOFs have been rapidly prepared. For example, in 2009, the efficient ultrasonic synthesis of HKUST-1 MOF was reported, obtaining smaller crystals (10-200 nm) than those synthesized using a conventional solvothermal method.[86]

1.2.3.6. Environmentally friendly synthesis

The growing awareness of energy efficiency, toxicity, and environmental impact of some chemical processes has led to the development of environmentally friendly synthesis methods.[87,88] Recently, efforts in synthetic chemistry have focused on achieving less harmful methods and processes. Although the conventional synthesis of MOFs depends on the use of high boiling point organic solvents, such as N,N' dimethylformamide (DMF) or N,N' diethylformamide (DEF), industrial green synthesis avoids these solvents due to their toxicity. For this reason, many studies have been conducted to synthesize MOFs using water as a solvent under room temperature. However, many of the organic ligands are not soluble in water, which limits the synthesis of MOFs under these conditions. For example, the water solubility of terephthalic acid, which is probably the most widely used organic ligand, is practically insignificant (0.0017 g/100 mL at 25 °C).

To overcome this limitation, it has been proposed the use of water as a solvent under critical conditions, since, under these conditions, the dielectric constant of water decreases and the solubility of the organic ligand and the processes of crystallization/precipitation change completely,[88] allowing the solvation of organic ligands,[87] and so the use of alkaline salts of organic ligands.

1.3. Structural details of the studied metal-organic frameworks

1.3.1. MIL-125 type metal-organic framework

MIL-125 (*Matériauxs de l'Institute Lavoisier*), based on the coordination of titanium clusters with aromatic carboxylic acids, crystallizes in the orthorhombic space group I4/mmm. The highly porous titanium-based MOF structure is composed of basic $Ti_8O_8(OH)_4$-$(O_2C$-C_6H_5-$CO_2)_6$ units and is built from cyclic octamers composed for octahedral titanium units that share corners or edges (*Figure 1.4*). These octamers are connected to 12 other cyclic octamers through BDC ligands, giving rise to a porous three-dimensional structure that has two types of cages, one octahedral (12.5 Å) and one tetrahedral (6 Å). These cages are accessible through 6 Å windows (*Figure 1.5*).[89-91]

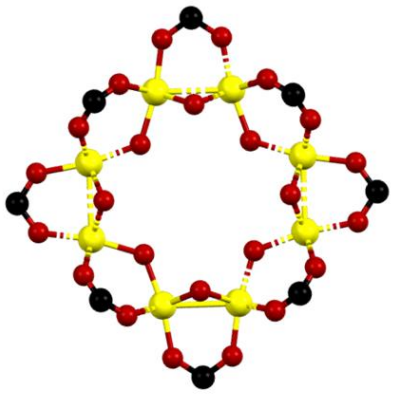

Figure 1.4. Secondary building unit of the MIL-125 type metal-organic framework. Carbon, oxygen, and titanium atoms are shown in black, red, and yellow, respectively.

MIL-125-NH_2 is isostructural to MIL-125 with smaller octahedral (10.7 Å) and tetrahedral (4.7 Å) cages and can be prepared by replacing H_2BDC with 2-aminoterephthalic acid (H_2BDC-NH_2).

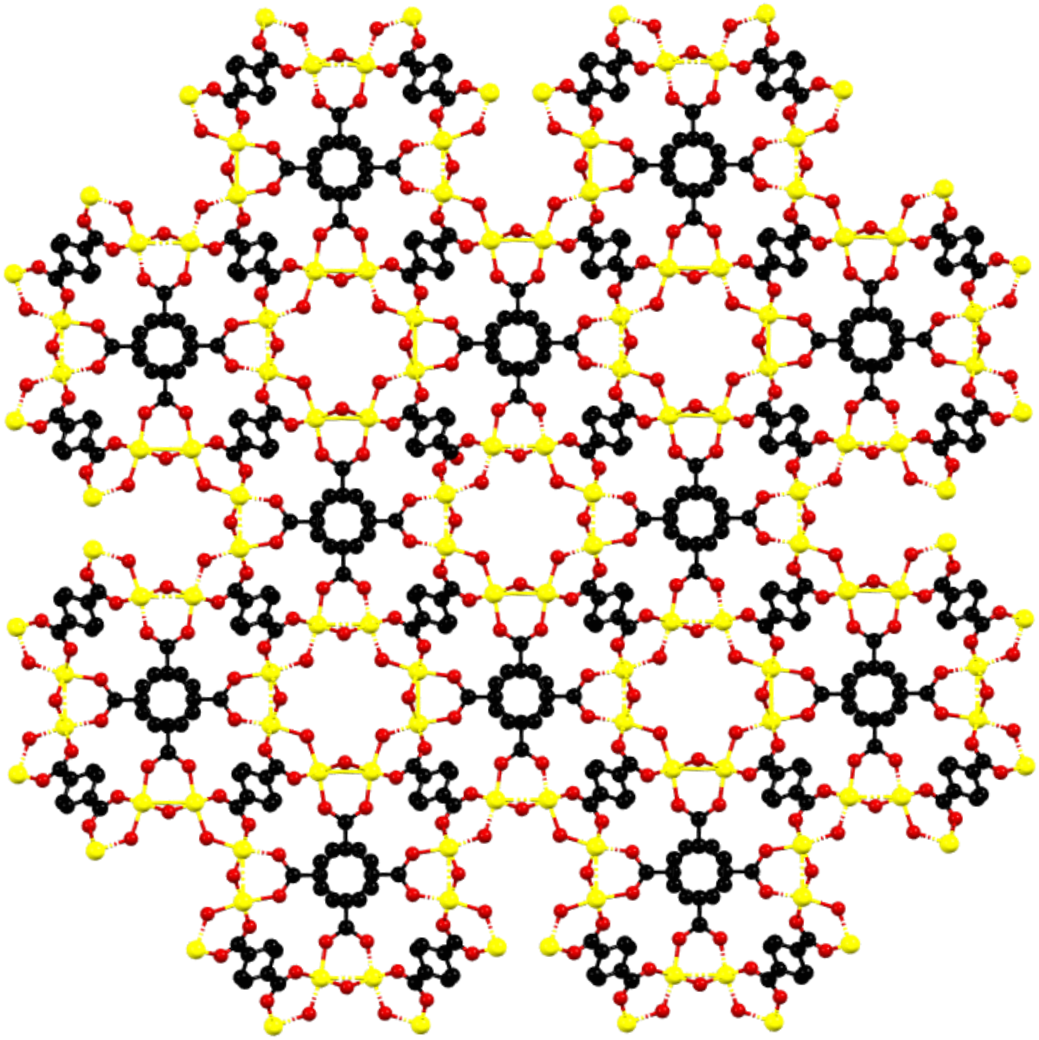

Figure 1.5. Structure of the MIL-125 type metal-organic framework. Carbon, oxygen, and titanium atoms are represented in black, red and yellow, respectively.

The high surface area of these MOFs and the presence of accessible -OH and -NH_2 groups on the clusters and on the linkers, respectively, make them good candidates for adsorption, separation, and catalysis applications. For example, Vermoortele et al. reported that MIL-125-NH_2 shows high p-xylene selectivity in the separation of isomer mixtures in the liquid phase,[92] while Anjum et al. investigated it for CO_2 separations from biogas and natural gas.[93]

1.3.2. NTU-9 type metal-organic framework

NTU-9 metal-organic framework, based on the coordination of titanium (IV) with 2,5-dihydroxyterephtalic acid (DOBDC) ligands, crystallizes in the trigonal space group P-31c. In this structure the titanium atom is octahedrally coordinated with six oxygen atoms from hydroxide

and carboxylate groups (*Figure 1.6*). The connection between Ti(IV) atoms and DOBDC linkers forms two dimensional (2D) honeycomb-like layers, which are stacked along the c-axis (*Figure 1.7*). The framework presents one dimensional (1D) channels about 11 Å × 11 Å, which are similar to the 1D channels of the MOF-74 structure.[94]

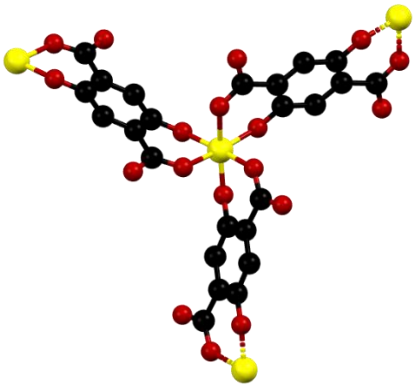

Figure 1.6. Secondary building unit of the NTU-9 type metal-organic framework. Carbon, oxygen, and titanium atoms are shown in black, red, and yellow, respectively.

Due to its photoelectrochemical properties, NTU-9 has been used as visible light photocatalyst for the degradation of pollutants[95] and for luminescent sensing.[96]

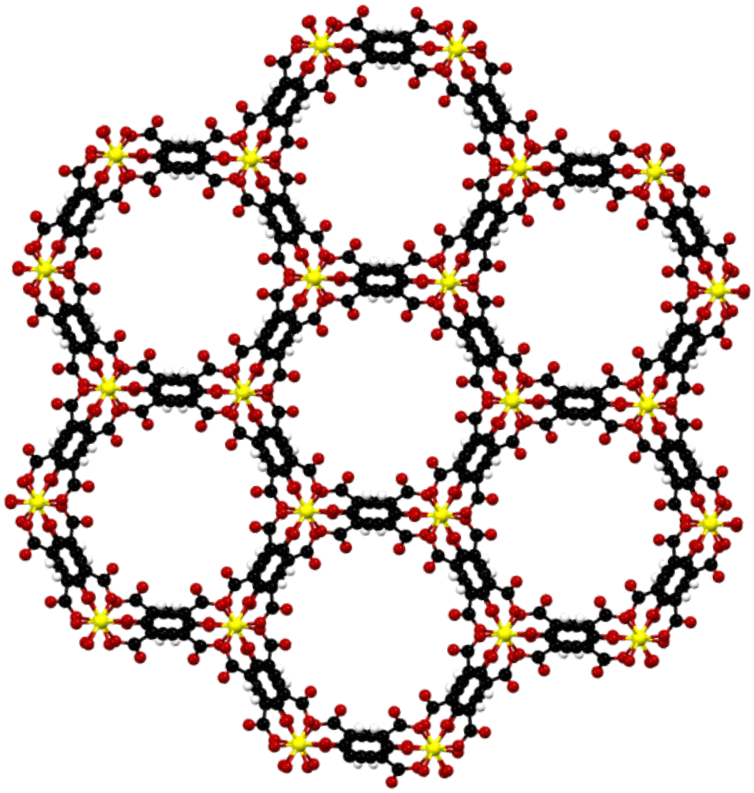

Figure 1.7. Structure of the NTU-9 type metal-organic framework. Carbon, oxygen, and titanium atoms are represented in black, red, and yellow, respectively.

1.3.3. MIL-100 type metal-organic framework

The metal-organic frameworks of the MIL-100 family have a zeotype structure and crystallise in the cubic system (space group Fd-$\bar{3}$m). MIL-100 MOFs formed by different metals such as Cr, Al, V, Sc, Ti or Fe have been described, being the MIL-100-Fe the most outstanding due to its low toxicity, low cost and water stability.[97,98]

The structure of MIL-100-Fe consists of $[Fe_3O(OH)(H_2O)_2]^{6+}$ iron clusters, in which the iron octahedra share a common μ_3-O-type vertex, linked by benzene-1,3,5-tricarboxylate (H_3BTC) ligands (*Figure 1.8*).[99]

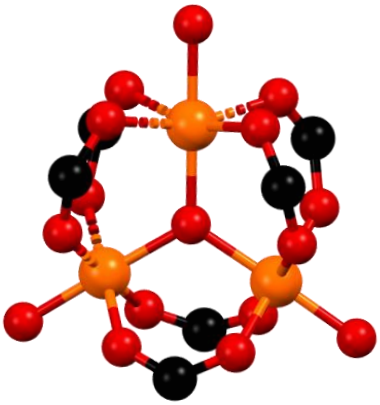

Figure 1.8. Secondary building unit of the MIL-100 type metal-organic framework. Carbon, oxygen, and iron atoms are shown in black, red, and orange, respectively.

The resulting structure has two types of mesoporous cavities with an internal diameter of 25 and 29 Å in a 2:1 ratio. The access to the smaller cavities is through pentagonal windows with an approximate diameter of 5.5 Å, while the larger cavity can be accessed through the same pentagonal windows as well as through hexagonal windows with an approximate diameter of 8.6 Å (*Figure 1.9*).

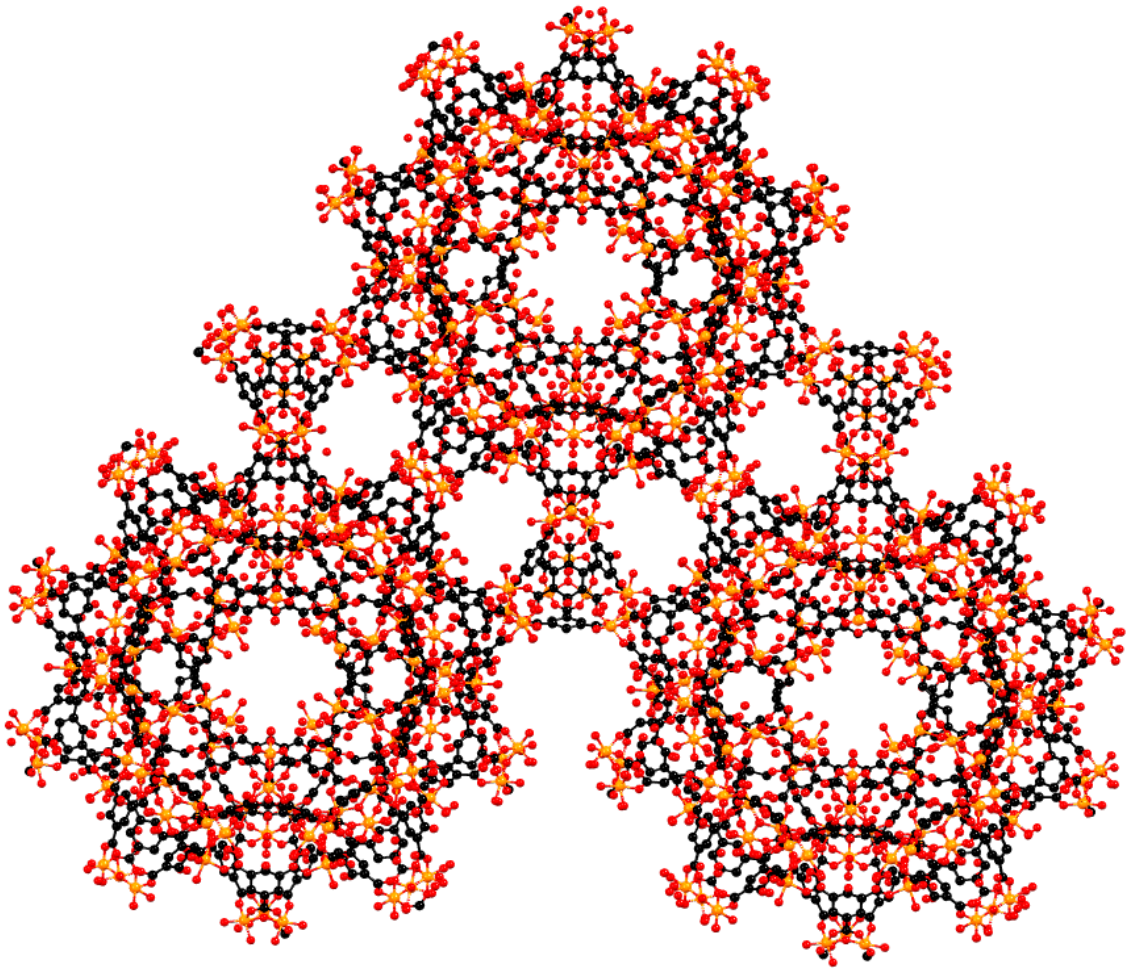

Figure 1.9. Structure of the MIL-100. Carbon, oxygen, and iron atoms are represented in black, red, and orange, respectively.

The structure has solvent molecules coordinated to the metal centers. As mentioned above, these molecules can be removed by heat treatment without altering the structure, giving rise to coordinatively unsaturated metal ions, which are available for covalent coordination with other molecules.

1.4. Materials derived from metal-organic frameworks

Thanks to their unique ordered porous structure, high surface area and versatility, MOFs have become interesting precursors for the synthesis of new porous materials, among which stands out the preparation of porous carbons and metal oxides.[100,101]

The controlled heating of MOFs at high temperature under an inert or oxidizing atmosphere results in the formation of nanoarchitectured carbons or metal oxides, respectively (*Figure 1.10*). In the first case, the MOF acts simultaneously as carbon source and template because the organic ligands turn into a porous carbon and the metal centers of the MOF aggregate and distribute on the carbon as metal or metal oxide particles.[102] The obtained carbons maintain the morphology of the pure MOF, show active sites and high specific surface areas and porosity, with the advantage, over the precursor MOF, of being chemically more stable. Furthermore, the metal particles distributed in the carbonaceous structure can provide new properties to the material, act as precursor for the preparation of hybrid materials or be removed to increase the porosity of the carbon.[103-106] All these characteristics make MOF-derived carbons suitable materials for a wide range of applications, such as removal of pollutants,[107] gas storage[108] and catalysis.[109]

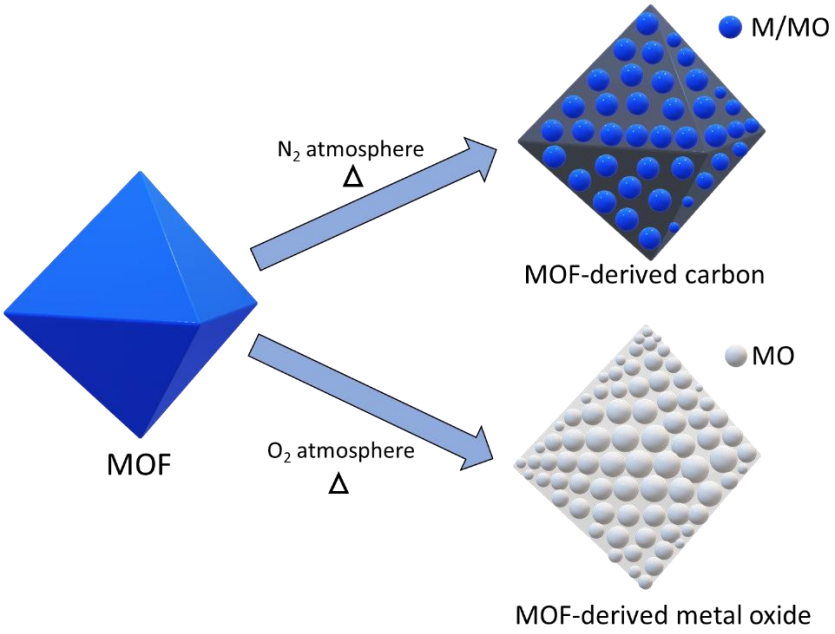

Figure 1.10. Schematic process for the preparation of MOF-derived materials.

If the MOFs is heated under air/oxygen atmosphere nanostructured metal oxides are obtained, due to the oxidation of metal centers and the release of CO_2 and NO_x from the decomposition of organic ligands during thermal treatment (*Figure 1.10*). The so prepared metal oxides also retain the morphology of the precursor MOF, show high surface area and can be doped with heteroatoms coming from the linker.[110] Currently, following this thermal treatment, different porous metal oxides such as Fe_2O_3,[111] Co_3O_4,[112] TiO_2[113] and CuO[114] have been synthesized and applied in lithium-ion batteries and as electrochemical capacitors (ECs), among other applications.

1.5. Bibliographic references

1. Çeçen F.; Aktaş, Ö. (2011). Water and wastewater treatment: Historical perspective of activated carbon adsorption and its integration with biological processes in activated carbon for water and wastewater treatment (pp. 1-11). *Wiley-VCH Verlag GmbH & Co*. KGaA.

2. Stoquart, C.; Servais, P.; Bérubé, P.R.; Barbeau, B. (2012). Hybrid membrane processes using activated carbon treatment for drinking water: A review. *J. Membr. Sci.*, *411-412*, 1-12.

3. Korotta-Gamage, S.M.; Sathasivan, A. (2017). A review: Potential and challenges of biologically activated carbon to remove natural organic matter in drinking water purification process. *Chemosphere*, *167*, 120-138.

4. Roegiers, J.; Denys, S. (2021). Development of a novel type activated carbon fiber filter for indoor air purification. *Chem. Eng. J.*, *417*, 128109.

5. Maximoff, S.N.; Mittal, R.; Kaushik, A.; Dhau, J.S. (2022). Performance evaluation of activated carbon sorbents for indoor air purification during normal and wildfire events. *Chemosphere*, *304*, 135314.

6. Maesen, T.; Marcus, B. (2001). Introduction to zeolite science and practice (pp. 1-9). *Elsevier*.

7. Liu, S.; Han, X.; Chai, Y.; Wu, G.; Li, W.; Li, J.; da Silva, I.; Manuel, P.; Cheng, Y.; Daemen, L. L.; Ramirez-Cuesta, A.J.; Shi, W.; Guan, N.; Yang, S.; Landong, L. (2021). Efficient separation of acetylene and carbon dioxide in a decorated zeolite. *Angew. Chem. Int. Ed.*, *60*, 6526-6532.

8. Dong, J.; Lin, Y. S.; Liu, W. (2000). Multicomponent hydrogen/hydrocarbon separation by MFI-type zeolite membranes. *AIChE J.*, *46*, 1957-1966.

9. Bareschino, P.; Mancusi, E.; Forgiones, A.; Pepe, F. (2020). Biogas purification on Na-X Zeolite: Experimental and numerical results. *Chem. Eng. Sci.*, *223*, 115744.

10. First, E.L.; Hasan, M.M.F; Floudas, C.A. (2014). Discovery of novel zeolites for natural gas purification through combined material screening and process optimization. *AIChE J.*, *60*, 1767-1785.

11. Zavareh, S.; Farrokhzad, Z.; Darvishi, F. (2018). Modification of zeolite 4A for use as an adsorbent for glyphosate and as an antibacterial agent for water. *Ecotoxicol. Environ. Saf.*, *155*, 1-8.

12. Servatan, M.; Zarrintaj, P.; Mahmodi, G.; Kim, S.-J.; Ganjali, M.R.; Saeb, M.R.; Mozafari, M. (2020). Zeolites in drug delivery: Progress, challenges and opportunities. *Drug Discov. Today*, *25*, 642-656.

13. Al-Jubouri, S.M.; Al-Batty, S.I.; Senthilnathan, S.; Sihanonth, N.; Sanglura, L.; Shan, H.; Holmes, S.M. (2021). Utilizing Faujasite-type zeolites prepared from waste aluminium foil for competitive ion-exchange to remove heavy metals from simulated wastewater. *Desalination Water Treat.*, *231*, 166-181.

14. Sun, Q.; Wang, N.; Yu, J. (2021). Advances in catalytic applications of zeolite-supported metal catalysts. *Adv. Mater.*, *33*, 2104442.

15. Yaghi, O.M.; Li, G. (1995). Mutually interpenetrating sheets and channels in the extended structure of [Cu(4,4'-bpy)Cl]. *Angew. Chem. Int. Ed., 34*, 207-209.

16. James, S.L. (2003). Metal-organic frameworks. *Chem. Soc. Rev.*, *32*, 276-288.

17. Zhou, H.C.; Long, J.R.; Yaghi, O.M. (2012). Introduction to metal-organic frameworks. *Chem. Rev.*, *112*, 673-674.

18. Zhou, H.C.; Kitagawa, S. (2014). Metal-organic frameworks (MOFs). *Chem. Soc. Rev.*, *43*, 5415-5418.

19. Moghadam, P.Z.; Li, A.; Wiggin, S.B.; Tao, A.; Maloney, A.G.P.; Wood, P.A.; Ward, S.C.; Fairen-Jimenez, D. (2017). Development of a Cambridge Structural Database subset: A collection of metal-organic frameworks for past, present, and future. *Chem. Mater.*, *29*, 2618-2625.

20. Martí-Gastaldo, C. (2016). Redes metal-orgánicas basadas en oligopéptidos. *An. Quím.*, *112*, 59-68.

21. Diring, S.; Furukawa, S.; Takashima, Y.; Tsuruoka, T.; Kitagawa, S. (2010). Controlled multiscale synthesis of porous coordination polymer in nano/micro regimes. *Chem. Mater.*, *22*, 4531-4538.

22. Farha, O.K.; Eryazici, I.; Jeong, N.C.; Hauser, B.G.; Wilmer, C.E.; Sarjeant, A.A.; Snurr, R.Q.; Nguyen, S.T.; Yazaydin, A.O.; Hupp, J.T. (2012). Metal-organic framework materials with ultrahigh surface areas: Is the sky the limit? *J. Am. Chem. Soc.*, *134*, 15016-15023.

23. Murray, L.; Dinca, M.; Long, J. (2009). Hydrogen storage in metal-organic frameworks. *Chem. Soc. Rev.*, *38*, 1294-1314.

24. Gupta, M.; Vittal, J.J. (2021). Control of interpenetration and structural transformations in the interpenetrated MOFs. *Coord. Chem. Rev.*, *435*, 213789.

25. Jiang, H.; Makal, T.A.; Zhou, H. (2013). Interpenetration control in metal-organic frameworks for functional applications. *Coord. Chem. Rev.*, *257*, 2232-2249.

26. Kholdeeva, O.A.; Skobelev, I.Y.; Ivanchikova, I.D.; Kovalenko, K.A.; Fedin, V.P.; Sorokin, A.B. (2014). Hydrocarbon oxidation over Fe- and Cr-containing metal-organic frameworks MIL-100 and MIL-101–a comparative study. *Catal. Today*, *238*, 54-61.

27. Van de Voorde, B.; Boulhout, M.; Vermoortele, F.; Horcajada, P.; Cunha, D.; Lee, J.S.; Chang, J.S.; Gibson, E.; Daturi, M.; Lavalley, J.C.; Vimont, A.; Beurroies, I.; De Vos, D.E. (2013). N/S-Heterocyclic contaminant removal from fuels by the mesoporous metal-organic framework MIL-100: The role of the metal ion. *J. Am. Chem. Soc.*, *135*, 9849-9857.

28. Zhao, D.; Wang, X.; Yue, L.; He, Y.; Chen, B. (2022). Porous metal-organic frameworks for hydrogen storage. *Chem. Commun.*, *58*, 11059-11078.

29. Chen, Y.; Ma, S. (2012). Microporous lanthanide metal-organic frameworks. *Inorg. Chem.*, *32*, 81-100.

30. Devic, T.; Serre, C. (2014). High valence 3p and transition metal based MOFs. *Chem. Soc. Rev.*, *43*, 6097-6115.

31. Ketrat, S.; Maihom, T.; Wannakao, S.; Probst, M.; Nokbin, S.; Limtrakul, J. (2017). Coordinatively unsaturated metal-organic frameworks $M_3(btc)_2$ (M = Cr, Fe, Co, Ni, Cu, and Zn) catalyzing the oxidation of CO by N_2O: Insight from DFT calculations. *Inorg. Chem.*, *56*, 14005-14012.

32. Ülkü K.; Anna G.; Leili E.; Maniya G.; Ali M.; Oliver W.; Christoph J. (2020). Coordinatively unsaturated metal sites (open metal sites) in metal-organic frameworks: design and applications. *Chem. Soc. Rev.*, *49*, 2751-2798.

33. DeCoste, J.B.; Peterson, G.W.; Schindler, B.J.; Killops, K.L.; Browe, M.A.; Mahle, J.J. (2013). The effect of water adsorption on the structure of the carboxylate containing metal-organic frameworks Cu-BTC, Mg-MOF-74, and UiO-66. *J. Mater. Chem. A*, *1*, 11922-11932.

34. Zhang, H.; Wu, S.; Tian, C.; Lin, Z.; Li, Z.; Lin, P.; Du. S. (2012). Two enantiomorphic 3D Zn (II)–carboxylate MOFs with double helical structures serving as a chiral source induced by hydrogen bonding. *CrystEngComm*, *14*, 4165-4167.

35. El Boutaybi, M.; Taleb, A.; Touzani, R.; Bahari, Z. (2020). Metal-organic frameworks based on pyrazole subunit for batteries applications: A systematic review. *Mater. Today Proc.*, *31*, S96-S102.

36. Xu, Y.; Liu, W.; Li, D.; Chen, H.; Lu, M. (2017). In situ synthesized 3D metal-organic frameworks (MOFs) constructed from transition metal cations and tetrazole derivatives: A family of insensitive energetic materials. *Dalton Trans.*, *46*, 11046-11052.

37. Wang, Z.; Cohen, S.M. (2009). Postsynthetic modification of metal-organic frameworks. *Chem. Soc. Rev.*, *38*, 1315-1329.

38. Tanabe, K.K.; Cohen, S.M. (2011). Postsynthetic modification of metal-organic frameworks—A progress report. *Chem. Soc. Rev.*, *40*, 498-519.

39. Wang, L.; Zhang, F.; Wang, C.; Li, Y.; Yang, J.; Li, L.; Li, J. (2020). Ethylenediamine-functionalized metal organic frameworks MIL-100(Cr) for efficient CO_2/N_2O separation. *Sep. Purif. Technol.*, *235*, 116219.

40. Trushina, D.B.; Sapach, A.Y.; Burachevskaia, O.A., Medvedev, P.V.; Khmelenin, D.N.; Borodina, T.N.; Soldatov, M.A.; Butova, V.V. (2022). Doxorubicin-loaded core-shell UiO-66@SiO_2 metal-organic frameworks for targeted cellular uptake and cancer treatment. *Pharmaceutics*, *14*, 1325.

41. Cheng, X.Q.; Li, S.; Bao, H.; Yang, X.; Li, Z.; Zhang, Y.; Wang, K.; Ma, J.; Ullah, A.; Shao, L. (2021). Poly(sodium-p-styrenesulfonate)-grafted UiO-66 composite membranes boosting highly efficient molecular separation for environmental remediation. *Adv. Compos. Hybrid Mater.*, *4*, 562-573.

42. Cui, Y.; Rimoldi, M.; Platero-Prats A.E.; Chapman K.W.; Hupp J.T.; Farha O.K. (2017). Stabilizing a vanadium oxide catalyst by supporting on a metal-organic framework. *ChemCatChem*, *10*, 1772-1777.

43. Li, Z.; Schweitzer, N.M.; League, A.B.; Bernales, V.; Peters, A.W.; Getsoian, A.B.; Wang, T.C.; Miller, J.T.; Vjunov, A.; Fulton, J.L.; Lercher, J.A.; Cramer, C.J.; Gagliardi, L.; Hupp, J.T.; Farha, O.K. (2016). Sintering-Resistant Single-Site nickel catalyst supported by metal-organic framework. *J. Am. Chem. Soc.*, *138*, 1977-1982.

44. McDonald, T.M.; D'Alessandro, D.M.; Krishna, R.; Long, J.R. (2011). Enhanced carbon dioxide capture upon incorporation of N,N'- dimethylethylenediamine in the metal-organic framework CuBTTri. *Chem. Sci.*, *2*, 2022-2028.

45. Cabello, C.P.; Berlier, G.; Magnacca, G.; Rumori, P.; Palomino, G.T. (2015). Enhanced CO_2 adsorption capacity of amine-functionalized MIL-100(Cr) metal-organic frameworks. *CrystEngComm*, *17*, 430-437.

46. Hasan, Z.; Choi, E.J.; Jhung, S.H. (2013). Adsorption of naproxen and clofibric acid over a metal-organic framework MIL-101 functionalized with acidic and basic groups. *Chem. Eng. J.*, *219*, 537-544.

47. Dapaah, M.F.; Liu, B.; Cheng, L. (2021). Adsorption of organic compounds from aqueous solution by pyridine-2-carboxaldehyde grafted MIL-101(Cr)-NH_2 metal-organic frameworks. *J. Environ. Chem. Eng.*, *9*, 105275.

48. Ning, H.; Yang, Z.; Yin, Z.; Wang, D.; Meng, Z.; Wang, C.; Zhang, Y.; Chen, Z. (2021). A novel strategy to enhance the performance of CO_2 adsorption separation: Grafting hyper-cross-linked polyimide onto composites of UiO-66-NH_2 and GO. *ACS Appl. Mater. Interfaces*, *13*, 17781-17790.

49. Chung, Y. M.; Kim, H.Y.; Ahn, W.S. (2014). Friedel-crafts acylation of p-Xylene over sulfonated zirconium terephthalates. *Catal. Lett.*, *144*, 817-824.

50. Devarajan, N.; Suresh, P. (2019). MIL-101-SO_3H metal-organic framework as a Brønsted acid catalyst in Hantzsch reaction: An efficient and sustainable methodology for one-pot synthesis of 1,4-dihydropyridine. *New J. Chem.*, *43*, 6806-6814.

51. Matsumoto, M.; Kitaoka, T. (2016). Ultraselective gas separation by nanoporous metal–organic frameworks embedded in gas-barrier nanocellulose films. *Adv. Mater.*, *28*, 1765-1769.

52. Jeazet, H.B.T.; Staudt, C.; Janiak, C. (2012). Metal-organic frameworks in mixed-matrix membranes for gas separation. *Dalton Trans.*, *41*, 14003-14027.

53. Qian, Q.; Asinger, P.A.; Lee, M.J.; Han, G.; Rodriguez, K.M.; Lin, S.; Benedetti, F.M.; Wu, A. X.; Chi, W.S.; Smith, Z.P. (2020). MOF-based membranes for gas separations. *Chem. Rev.*, *120*, 8161-8266.

54. Sule, R.; Mishra, A.K.; Nkambule, T.T. (2021). Recent advancement in consolidation of MOFs as absorbents for hydrogen storage. *Int. J. Energy Res.*, *45*, 12481-12499.

55. Suh, M.P.; Park, H.J.; Prasad, T.K.; Lim, D.W. (2012). Hydrogen storage in metal-organic frameworks. *Chem. Rev.*, *112*, 782-835.

56. Shet, S.P.; Shanmuga Priya, S.; Sudhakar, K.; Tahir, M. (2021). A review on current trends in potential use of metal-organic framework for hydrogen storage. *Int. J. Hydrog. Energy*, *46*, 11782-11803.

57. Trickett, C.A.; Helal, A.; Al-Maythalony, B.A.; Yamani, Z.H.; Cordova, K.E.; Yaghi, O.M. (2017). The chemistry of metal-organic frameworks for CO_2 capture, regeneration and conversion. *Nat. Rev. Mater.*, *2*, 17045.

58. Iqbal, B.; Saleem, M.; Arshad, S.N.; Rashid, J. (2019). One-pot synthesis of heterobimetallic metal-organic frameworks (MOFs) for multifunctional catalysis. *Chem. -Eur. J.*, *25*, 10490-10498.

59. Hu, M.L.; Safarifard, V.; Doustkhah, E.; Rostamnia, S.; Morsali, A.; Nouruzi, N.; Beheshti, S.; Akhbari, K. (2018). Taking organic reactions over metal-organic frameworks as heterogeneous catalysis. *Microporous Mesoporous Mater.*, *256*, 111-127.

60. Konnerth, H.; Matsagar, B.M.; Chen, S.S.; Prechtl, M.H.G.; Shieh, F.-K.; Wu, K.C.W. (2020). Metal-organic framework (MOF)-derived catalysts for fine chemical production. *Coord. Chem. Rev.*, *416*, 213319.

61. Lázaro, I.A.; Forgan, R.S. (2019). Application of zirconium MOFs in drug delivery and biomedicine. *Coord. Chem. Rev.*, *380*, 230-259.

62. Sun, Y.; Zheng, L.; Yang, Y.; Qian, X.; Fu, T.; Li, X.; Yang, Z.; Yan, H.; Cui, C.; Tan, W. (2020). Metal-organic framework nanocarriers for drug delivery in biomedical applications. *Nano-Micro Lett.*, *12*, 103.

63. Bieniek, A.; Terzyk, A.P.; Wiśniewski, M.; Roszek, K.; Kowalczyk, P.; Sarkisov, L.; Keskin, S.; Kaneko, K. (2021). MOF materials as therapeutic agents, drug carriers, imaging agents and biosensors in cancer biomedicine: Recent advances and perspectives. *Prog. Mater. Sci.*, *117*, 100743.

64. Liu, X.; Zhou, Y.; Zhang, J.; Tang, L.; Luo, L.; Zeng, G. (2017). Iron containing metal-organic frameworks: Structure, synthesis, and applications in environmental remediation. *ACS Appl. Mater. Interfaces*, *9*, 20255-20275.

65. Dhaka, S.; Kumar, R.; Deep, A.; Kurade, M.B.; Ji, S.W.; Jeon, B. H. (2019). Metal-organic frameworks (MOFs) for the removal of emerging contaminants from aquatic environments. *Coord. Chem. Rev*, *380*, 330-352.

66. Zhang, S.; Wang, J.; Zhang, Y.; Ma, J.; Huang, L.; Yu, S.; Chen, L.; Song, G.; Qiu, M.; Wang, X. (2021). Applications of water-stable metal-organic frameworks in the removal of water pollutants: A review. *Environ. Pollut.*, *291*, 118076.

67. Zhang, X.; Wang, B.; Alsalme, A.; Xiang, S.; Zhang, Z.; Chen, B. (2020). Design and applications of water-stable metal-organic frameworks: status and challenges. *Coord. Chem. Rev.*, *423*, 213507.

68. Li, X.; Xing, J.; Chang, C.; Wang, X.; Bai, Y.; Yan, X.; Liu, H. (2014). Solid-phase extraction with the metal-organic framework MIL-101(Cr) combined with direct analysis in real time mass spectrometry for the fast analysis of triazine herbicides. *J. Sep. Sci.*, *37*, 1489-1495.

69. Fang, Y.; Yang, Z.; Li, H.; Liu, X. (2020). MIL-100(Fe) and its derivatives: from synthesis to application for wastewater decontamination. *Environ. Sci. Pollut. Res.*, *27*, 4703-4724.

70. Ahmadijokani, F.; Molavi, H.; Rezakazemi, M.; Tajahmadi, S.; Bahi, A.; Ko, F.; Aminabhavi, T. M.; Li, J.-R.; Arjmand, M. (2022). UiO-66 metal-organic frameworks in water treatment: A critical review. *Prog. Mater. Sci.*, *125*, 100904.

71. Lin, K.S.; Adhikari, A.K.; Ku, C.N.; Chiang, C.L.; Kuo, H. (2012). Synthesis and characterization of porous HKUST-1 metal organic frameworks for hydrogen storage. *Int. J. Hydrogen Energy*, *37*, 13865-13871.

72. Wang, Q.; Sun, Y.; Li, S.; Zhang, P.; Yao, Q. (2020). Synthesis and modification of ZIF-8 and its application in drug delivery and tumour therapy. *RSC Adv.*, *10*, 37600-37620.

73. Garibay, S.J.; Cohen, S.M. (2010). Isoreticular synthesis and modification of frameworks with the UiO-66 topology. *ChemComm*, *46*, 7700-7702.

74. Zhu, X.; Li, B.; Yang, J.; Li, Y.; Zhao, W.; Shi, J.; Gu, J. (2015). Effective adsorption and enhanced removal of organophosphorus pesticides from aqueous solution by Zr-Based MOFs of UiO-67. *ACS Appl. Mater. Interfaces*, *7*, 223-231.

75. Horcajada, P.; Surblé, S.; Serre, C.; Hong, D.Y.; Seo, Y.K.; Chang, J.S.; Grenèche, J.M.; Margiolaki, I.; Férey, G. (2007). Synthesis and catalytic properties of MIL-100(Fe), an iron(III) carboxylate with large pores. *ChemComm*, *27*, 2820-2822.

76. Banerjee, R.; Phan, A.; Wang, B.; Knobler, C.; Furukawa, H.; O'Keeffe, M.; Yaghi, O.M. (2008). High-Throughput synthesis of zeolitic imidazolate frameworks and application to CO_2 capture. *Science*, *319*, 936-939.

77. Klinowski, J.; Paz, F.A.A.; Silva, P.; Rocha, J. (2011). Microwave-assisted synthesis of metal-organic frameworks. *Dalton Trans.*, *40*, 321-330.

78. Zeng, X.; Hu, X.; Song, H.; Xia, G.; Shen, Z.-Y.; Yu, R.; Moskovits, M. (2021). Microwave synthesis of zeolites and their related applications. *Microporous Mesoporous Mater.*, *323*, 111262.

79. Kappe, C.O. (2004). Controlled microwave heating in modern organic synthesis. *Angew. Chem. Int. Ed.*, *43*, 6250-6284.

80. Ni, Z.; Masel, R.I. (2006). Rapid production of metal-organic frameworks via microwave-assisted solvothermal synthesis. *J. Am. Chem. Soc.*, *128*, 12394-12395.

81. Campagnol, N.; van Assche, T.; Boudewijns, T.; Denayer, J.; Binnemans, K.; de Vos, D.; Fransaer, J. (2013). High pressure, high temperature electrochemical synthesis of metal-organic frameworks: Films of MIL-100 (Fe) and HKUST-1 in different morphologies. *J. Mater. Chem. A*, *1*, 5827-5830.

82. Van Assche, T.R.C.; Desmet, G.; Ameloot, R.; de Vos, D.E.; Terryn, H.; Denayer, J.F.M. (2012). Electrochemical synthesis of thin HKUST-1 layers on copper mesh. *Microporous Mesoporous Mater.*, *158*, 209-213.

83. Singh, N.K.; Hardi, M.; Balema, V.P. (2013). Mechanochemical Synthesis of an yttrium based metal-organic framework. *Chem. Commun.*, *49*, 972-974.

84. Kim, J.; Yang, S.T.; Choi, S.B.; Sim, J.; Kim, J.; Ahn, W.S. (2011). Control of catenation in CuTATB-n metal-organic frameworks by sonochemical synthesis and its effect on CO_2 adsorption. *J. Mater. Chem.*, *21*, 3070-3076.

85. James, S.L.; Adams, C.J.; Bolm, C.; Braga, D.; Collier, P.; Frišcic, T.; Grepioni, F.; Harris, K.D. M.; Hyett, G.; Jones, W.; Krebs, A.; Mack, J.; Maini, L.; Orpen, A.G.; Parkin, I.P.; Shearouse, W.C.; Steed, J.W.; Waddell, D.C. (2012). Mechanochemistry: opportunities for new and cleaner synthesis. *Chem. Soc. Rev.*, *41*, 413-447.

86. Li, Z.Q.; Qiu, L.G.; Xu, T.; Wu, Y.; Wang, W.; Wu, Z.Y.; Jiang, X. (2009). Ultrasonic synthesis of the microporous metal-organic framework $Cu_3(BTC)_2$ at ambient temperature and pressure: An efficient and environmentally friendly method. *Mater. Lett.*, *63*, 78-80.

87. Ibarra, I.A.; Bayliss, P.A.; Pérez, E.; Yang, S.; Blake, A.J.; Nowell, H.; Allan, D.R.; Poliakoff, M.; Schröder, M. (2012). Near-critical water, a cleaner solvent for the synthesis of a metal organic framework. *Green Chem.*, *14*, 117-122.

88. Sánchez-Sánchez, M.; Getachew, N.; Díaz, K.; Díaz-García, M.; Chebude, Y.; Díaz, I. (2015). Synthesis of metal-organic frameworks in water at room temperature: salts as linker sources. *Green Chem.*, *17*, 1500-1509.

89. Dan-Hardi, M.; Serre, C.; Frot, T.; Rozes, L.; Maurin, G.; Sanchez, C.; Férey G. (2009). A new photoactive crystalline highly porous titanium(IV) dicarboxylate. *J. Am. Chem. Soc.*, *131*, 10857-10859.

90. Zlotea, C.; Phanon, D.; Mazaj, M.; Heurtaux, D.; Guillerm, V.; Serre, C.; Horcajada, P.; Devic, T.; Magnier, E.; Cuevas, F.; Férey, G.; Llewellynm P.L.; Latroche, M. (2011). Effect of NH_2 and CF_3 functionalization on the hydrogen sorption properties of MOFs. *Dalton Trans.*, *40*, 4879-4881.

91. Kim, S.-N.; Kim, J.; Kim, H.-Y.; Cho, H.-Y.; Ahn, W.-S. (2013). Adsorption/catalytic properties of MIL-125 and NH_2-MIL-125. *Catal. Today*, *204*, 85-93.

92. Vermoortele, F.; Maes, M.; Moghadam, P.Z.; Lennox, M.J.; Ragon, F.; Boulhout, M.; Biswas, S.; Laurier, K.G.M.; Beurroies, I.; Denoyel, R.; Roeffaers, M.; Stock, N.; Düren, T.; Serre, C.; De Vos, D.E. (2011). p-Xylene-selective metal-organic frameworks: a case of topology-directed selectivity. *J. Am. Chem. Soc.*, *133*, 18526-18529.

93. Anjum, M.W.; Bueken, B.; De Vos, D.; Vankelecom, I.F.J. (2016). MIL-125(Ti) based mixed matrix membranes for CO_2 separation from CH_4 and N_2. *J. Membr. Sci.*, *502*, 21-28.

94. Gao, J.; Miao, J.; Li, P.-Z.; Teng, W.Y.; Yang, L.; Zhao, Y.; Liu, B.; Zhang, Q. (2014). A p-type Ti(IV)-based metal-organic framework with visible-light photo-response. *Chem. Commun.*, *50*, 3786-3788.

95. Howe, J.D.; Morelock, C.R.; Jiao, Y.; Chapman, K.W.; Walton, K.S.; Sholl, D.S. (2017). Understanding structure, metal distribution, and water adsorption in mixed-metal MOF-74. *J. Phys. Chem. C*, *121*, 627-635.

96. Xu, H.; Gao, J.; Qian, X.; Wang, J.; He, H.; Cui, Y.; Yang, Y.; Wang, Z.; Qian, G. (2016). Metal-organic framework nanosheets for fast-response and highly sensitive luminescent sensing of Fe^{3+}. *J. Mater. Chem. A*, *4*, 10900-10905.

97. Fang, Y.; Yang, Z.; Li, H.; Liu, X. (2020). MIL-100(Fe) and its derivatives: from synthesis to application for wastewater decontamination. *Environ. Sci. Pollut. Res.*, *27*, 4703-4724.

98. Gao C., Chen S., Quan X., Yu H., Zhang Y. (2017). Enhanced Fenton-like catalysis by iron-based metal organic frameworks for degradation of organic pollutants. *J. Catal.*, *356*, 125-132.

99. Bezverkhyy, I.; Weber, G.; Bellat, J.P. (2016). Degradation of fluoride-free MIL-100(Fe) and MIL-53(Fe) in water: Effect of temperature and pH. *Microporous Mesoporous Mater.*, *219*, 117-124.

100. Wang, L.; Zhu, Y.; Du, C.; Ma, X.; Cao, C. (2020). Advances and challenges in metal-organic framework derived porous materials for batteries and electrocatalysis. *J. Mater. Chem. A*, *8*, 24895-24919

101. Chen, Y.-Z.; Zhang, R.; Jiao, L.; Jiang, H.-L. (2018). Metal-organic framework-derived porous materials for catalysis. *Coord. Chem. Rev.*, *362*, 1-23.

102. Tang, J.; Salunkhe, R.R.; Liu, J.; Torad, N.L.; Imura, M.; Furukawa, S.; Yamauchi, Y. (2015). Thermal conversion of core-shell metal-organic frameworks: A new method for selectively functionalized nanoporous hybrid carbon. *J. Am. Chem. Soc.*, *137*, 1572-1580.

103. Wang, Y.C.; Li, W.B.; Zhao, L.; Xu, B.Q. (2016). MOF-derived binary mixed metal/metal oxide@carbon nanoporous materials and their novel supercapacitive performances. *Phys. Chem. Chem. Phys.*, *18*, 17941-17948.

104. Bhadra, B.N.; Jhung, S.H. (2018). Well-dispersed Ni or MnO nanoparticles on mesoporous carbons: preparation via carbonization of bimetallic MOF-74s for highly reactive redox catalysts. *Nanoscale*, *10*, 15035-15047.

105. Chen, J.J.; Chen, Y.T.; Raja, D.S., Kang, Y.H.; Tseng, P.C.; Lin, C.H. (2015). Metal-organic frameworks to metal/metal oxide embedded carbon matrix: Synthesis, characterization and gas sorption properties. *Materials*, *8*, 5336-5347.

106. Del Rio, M.; Palomino, G.T.; Cabello, C.P. (2020). Metal-organic framework@carbon hybrid magnetic material as an efficient adsorbent for pollutant extraction. *ACS Appl. Mater. Interfaces*, 12, 6419-6425.

107. Yu, F.; Bai, X.; Liang, M.; Ma, J. (2021). Recent progress on metal-organic framework-derived porous carbon and its composite for pollutant adsorption from liquid phase. *Chem. Eng. J.*, *405*, 126960.

108. Chen, S.; Li, Y.; Mi, L. (2020). Porous carbon derived from metal organic framework for gas storage and separation: The size effect. *Inorg. Chem. Commun.*, *118*, 107999.

109. Shen, Q.; Li, X.; Li, R.; Wu, Y. (2020). Application of metal-organic framework materials and derived porous carbon materials in catalytic hydrogenation. *ACS Sustain. Chem. Eng.*, *8*, 17608-17621.

110. Salunkhe, R.R.; Kaneti, Y.V.; Yamauchi, Y. (2017). Metal-organic framework-derived nanoporous metal oxides toward supercapacitor applications: Progress and prospects. *ACS Nano*, *11*, 5293-5308.

111. Xu, X.; Cao, R.; Jeong, S.; Cho, J. (2012). Spindle-like mesoporous α-Fe_2O_3 anode material prepared from MOF template for high-rate lithium batteries. *Nano Lett.*, *12*, 4988-4991.

112. Salunkhe, R.R.; Tang, J.; Kamachi, Y.; Nakato, T.; Kim, J.H.; Yamauchi, Y. (2015). Asymmetric supercapacitors using 3D nanoporous carbon and cobalt oxide electrodes synthesized from a single metal-organic framework. *ACS Nano*, *9*, 6288-6296.

113. Ma, J.; Liu, W.; Liang, X.; Quan, B.; Cheng, Y.; Ji, G.; Meng, W. (2017). Nanoporous TiO_2/C composites synthesized from directly pyrolysis of a Ti-based MOFs MIL-125(Ti) for efficient microwave absorption. *J. Alloys Compd.*, *728*, 138-144.

114. Banerjee, A.; Singh, U.; Aravindan, V.; Srinivasan, M.; Ogale, S. (2013). Synthesis of CuO nanostructures from Cu-based metal organic framework (MOF-199) for application as anode for Li-ion batteries. *Nano Energy*, *2*, 1158-1163.

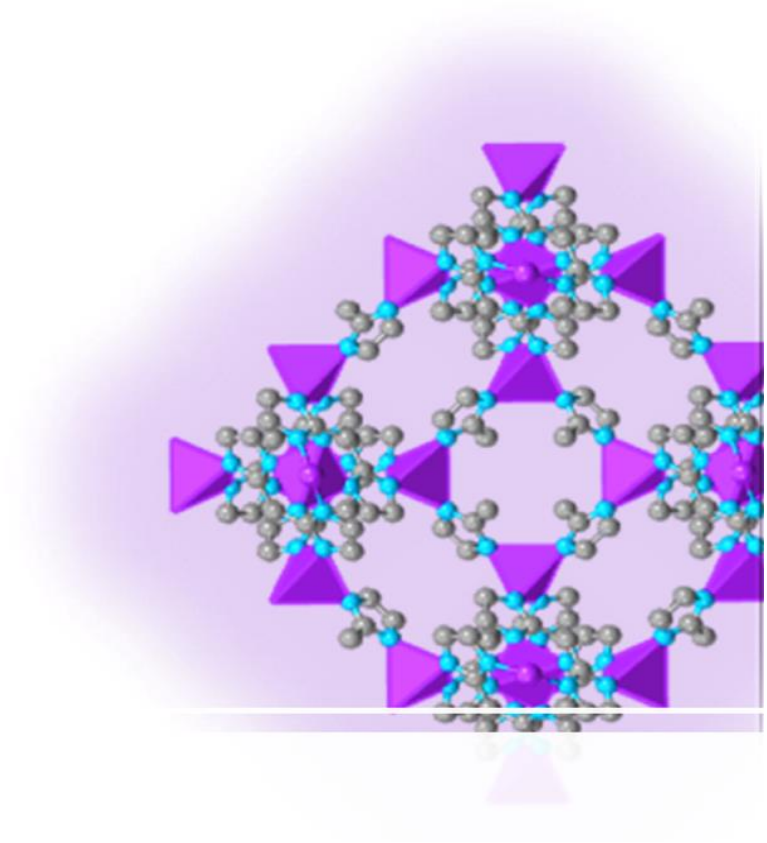

Chapter 2

State of the art and objectives

This Chapter provides a comprehensive overview of what has been done in the application of MOFs and derived materials for the removal of pollutants, as well as what should be further investigated, in order to formulate the main objectives of this thesis.

Chapter 2: State of the art and general objectives

2.1. State of the art

The degradation of the environment is one of the main problems facing humanity today. Rapid scientific and technological advances have allowed great developments for humanity, however they have also led to the alteration of the ecological balance of the planet and, as a result, caused harmful effects on the environment. From the 70s, society began to develop awareness of the need to protect the environment, and the concept of *Sustainable Development* is introduced. This term was first formulated in the Brundtland report (1987) and was defined as: "*To fulfil the needs of the present generations without compromising the possibilities of the future*".[1] According to this definition, sustainable development seeks the reconciliation between economic growth, natural resources, and society.

In order to achieve sustainable development, it is essential to reduce and control the pollution generated by citizens and to seek new alternatives of production through less harmful technologies, in combination with pressure from governments through more restrictive legislation. For this reason, industries have started to adapt their processes according to the recommendations of *Green Chemistry*.[2] This term was introduced by *Environmental Protection Agency* (EPA) in 1996 and aims at the design, development and implementation of processes and chemicals intended to reduce or eliminate dangerous substances from the environment.[3]

On this matter, water is an essential natural resource for all living beings and our planet. For this reason, the current anthropogenic pollution of water resources has become a serious global problem. At present, it is known that water contains a wide variety of substances that are harmful to human and environmental health, among which persistent organic compounds (POPs), such as herbicides, pesticides, phenolic compounds, and pharmaceutical compounds can be highlighted. In this context, the development of efficient and simple technologies capable of eliminating these contaminants and guarantee the quality standards of water is urgent. To achieve this objective, different strategies have been developed to eliminate the contaminants present in water, such as heterogeneous photocatalysis,[4,5] Fenton oxidation,[6] microwave-induced catalytic degradation,[7,8] electrochemical oxidation[9,10] and adsorption.[11,12]

Adsorption, using porous materials as adsorbents, due to its efficiency, low cost, simplicity and no generation of harmful secondary products, is presented as a promising strategy for water decontamination. Consequently, research is focused on the development of new

adsorbent materials with greater adsorption capacity, selectivity, stability and regenerability.[13,14]

The excellent properties of MOFs, such as large specific surface area and high porosity, which facilitates the diffusion of different molecules to binding sites, and their high variety, in terms of topology and composition, make them promising materials for the extraction of organic pollutants. For instance, ZIF-67, MIL-100 and UiO-66 MOFs have been efficiently used for the extraction of different pharmaceuticals,[15-18] dyes[19-21] and phenolic compounds.[22,23] The adsorption of these pollutants by MOFs occurs through a number of different mechanisms, including electrostatic interactions, hydrogen bonding, acid-base interactions, $\pi-\pi$ interactions, or a combination of them (*Figure 2.1*). Previous studies have shown that the incorporation of functional groups in MOFs, via functionalization of their organic linkers and/or metal nodes, enhances these interactions, thus improving their selectivity and adsorption capacity.[24,25] For example, it has been shown that the incorporation of amine groups in the coordinatively unsaturated metal centers of the MIL-101 MOF significantly increases its naproxen and oxytetracycline adsorption capacity.[26,27] A similar approach was used by Dapaah et al. who functionalized MIL-101 MOF with pyridine-2-carboxaldehyde, thus achieving an improvement in its extraction capacity of bisphenol A.[28] Other examples are the preparation of carboxylic-acid-functionalized UiO-66-NH_2 for the extraction of triclosan[29] and the use of MIL-101(Cr) with nitro groups for the removal of methylenedianiline and p-phenylenediamine,[30] in which the extraction capacity was increased by hydrogen bonding between the MOF and the pollutant.

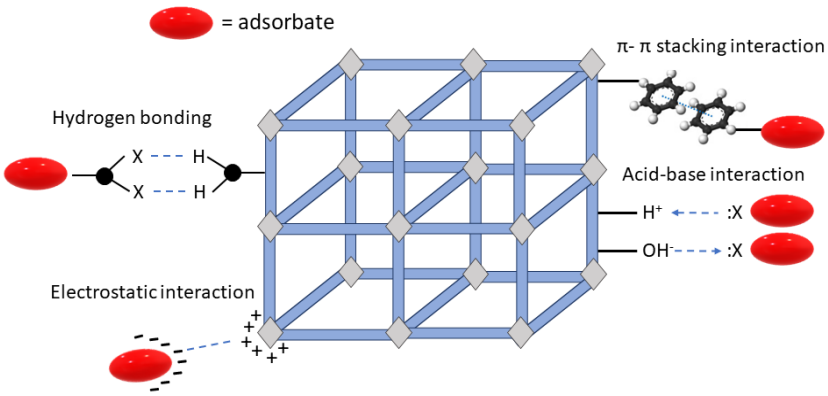

Figure 2.1. Several plausible mechanisms for the adsorption of pollutants over MOFs.

For the practical application of MOFs as adsorbents, it is important to study their adsorption capacity and kinetics, which depend on their chemical, textural and morphological properties, as well as their stability. Besides thermal stability, another important aspect to

consider in the use of MOFs as adsorbents is their chemical stability. Many of the coordination bonds in MOFs are reversible, which means that they are more easily attacked by molecules with stronger coordination capabilities, such as water molecules, causing structural collapse. In this regard, stable porous carbons have been prepared by a facile and single-step calcination procedure under an inert atmosphere, without the need of any additional carbon precursors using MOFs as both, templates and carbon precursors.[31-34] These materials, due to their remarkable high surface area, thermal and chemical stability, and their tendency to establish favourable interactions with the aromatic rings of organic compounds, have become very promising materials for water treatment.[35,36] For instance, porous carbons derived from ZIF-8,[37] ZIF-67,[38] MOF-74[34] and MAF-6[39] have been successfully used for the removal of pharmaceuticals, dyes, insecticides and hydrocarbons, among others.

Another efficient procedure for the treatment of polluted water is the degradation of environmental contaminants by heterogeneous photocatalysis, which allows the transformation of different compounds into less toxic species using a semiconductor as photocatalysts.[40,41] The photocatalytic process starts when the semiconductor material absorbs radiant energy greater than or equal to the bandgap energy (Eg). This fact causes the transfer of electrons (e^-) from the valence band (VB) to the conduction band (CB), giving rise to the formation of electron-hole pairs (e^-/h^+).[42,43] The photogenerated e^-/h^+ pairs allow the initiation of a series of redox reactions, which aim to produce hydroxyl radicals (·OH) with sufficient oxidation potential to degrade, quickly and non-selectively, a wide spectrum of pollutants adsorbed on the surface of the catalyst (*Figure 2.2*).

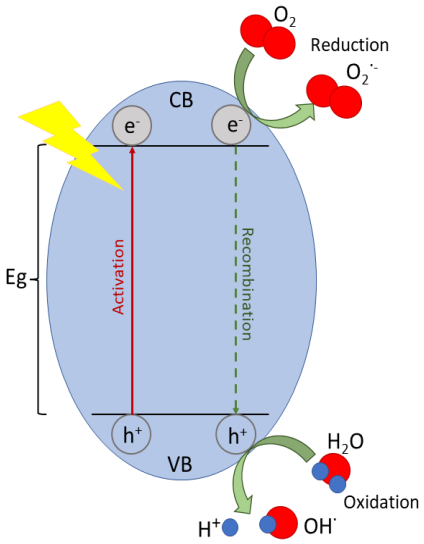

Figure 2.2. Schematic representation of the formation/production of radicals on the surface of a semiconductor.

Among the different semiconductors, such as TiO_2,[44,45] ZnO,[46,47] CuO,[48] WO_3,[49] and Fe_2O_3,[50] that can be applied to degrade organic contaminants, due to their high photochemical stability and low toxicity, TiO_2 and ZnO oxides are the most used. However, the application of these oxides for photocatalytic degradation has some drawbacks, such as high band gap, quick recombination of e^- and h^+ and incomplete mineralization of the pollutants. In order to overcome these limitations, new porous metal oxides have been prepared using different methods.[51,52] In this context, recently, MOFs, due to their highly ordered pore structure, large surface area and chemical versatility, have been used as precursors for the preparation of porous metal oxides by a simple oxidation procedure.[53-55] For example, metal oxides derived from zinc-based MOFs, such as ZIF-8[56,57] and MOF-5,[58,59] have shown excellent performance for the degradation of a variety of organic dyes. The preparation of TiO_2 derived from MOFs has focused on the use of MIL-125 type MOF as a precursor. For example, a carbon-doped TiO_2 derived from MIL-125 has been successfully applied for the photodegradation of bisphenol A under visible light radiation,[60] while Li et al. also synthesized an anatase/rutile mixed phase TiO_2 through the pyrolysis of MIL-125 for the degradation of nitrobenzene[61] and rhodamine B.[62]

One of the most critical points when using powdered materials for the removal of environmental pollutants is the separation of the adsorbent or catalyst from the sample medium, which usually requires laborious and time-consuming filtration (or centrifugation) procedures with the consequent loss of solid particles. An interesting strategy to improve this step is the incorporation of the porous material on supports such as fibers, monoliths, sponges, and membranes, which facilitates the material recovery and its applicability. For instance, a polytetrafluoroethylene (PTFE) double layer membrane has been modified with ZIF-8 MOF and tested for the adsorption of progesterone from water.[63] Moreover, UiO-66 has been incorporated into porous polymer monoliths to enhance the chromatographic liquid separation of small molecules.[64] Prasetya et al. also described the growth of a polycrystalline layer of MOF-808 on the surface of a yttria-stabilised zirconia hollow fibre support and the application of the prepared hybrid material in the adsorption of diclofenac.[65] Other examples of the incorporation of porous materials on supports for the removal of pollutants are the growth of ZIF-8 MOF onto a melamine sponge for effective oil/water separation[66] and the use of a hybrid membrane composed of NH_2-MIL-88B MOF and graphene oxide for the degradation of methylene blue dye through a photo-Fenton process.[67]

3D printed supports have become a very promising alternative to conventional supports for the preparation of functional devices. 3D printing (or additive manufacturing) is a new manufacturing technology that allows the creation of three-dimensional objects by

superimposing successive layers of a given material. The main advantage of this technique is the high processability of the polymers used, since they can be easily moulded into any shape, which offers great opportunities for the development of new materials.[68,69] In this context, recently, the incorporation of MOFs into 3D printed supports, obtained by using different 3D-printing techniques such as stereolithography or fused deposition modelling, has led a new generation of highly customized devices with great potential in many fields, including gas adsorption,[70,71] energy storage,[72,73] catalysis[74] and pollutant removal.[75] However, although the possibilities of using 3D printing in this last field are enormous, they have been still barely exploited.

2.2. General objectives of the thesis project

The protection of the environment and the management of natural resources requires the development and improvement of technologies both to control parameters of environmental interest, as well as to eliminate contaminants present in the environment. Bearing this in mind and what has been discussed throughout this chapter, the main objective of this Doctoral Thesis is to develop new hybrid materials, based on metal-organic frameworks and derived materials, to evaluate their suitability towards the extraction and degradation of environmental pollutants. For the achievement of this main goal, three specific objectives have been set:

1. The synthesis and characterization of a porous carbon derived from MIL-125-NH_2 metal-organic framework, as well as the evaluation of its adsorption capacity for organic pollutants. Preparation of a hybrid membrane from the obtained carbon and study of its extraction and preconcentration capacity of toxic phenolic compounds present in plastics.

2. The preparation and characterization of a porous titanium oxide derived from the NTU-9 MOF and the evaluation of its use as a photocatalyst for the degradation of methylene blue dye. Obtention of a magnetic stirrer coated with the synthesized TiO_2 and study of its application in the photodegradation of the dye.

3. The grafting of a MIL-100-Fe MOF with aminomethane sulfonic acid, as well as the evaluation of its extraction capacity for the anti-inflammatory drug diclofenac.

Incorporation of the functionalized MIL-100-Fe onto a 3D printed column and the evaluation of the developed device for the extraction, preconcentration and analysis of low levels of pharmaceuticals in water samples.

2.3. Bibliographic references

1. Brundtland Report: <<Our common future>> (1987). Harlem, G., United Nations Organization (ONU).

2. Anastas, P.; Eghbali, N. (2010). Green chemistry: Principles and practice. *Chem. Soc. Rev.*, *39*, 301-312.

3. The Presidential Green Chemistry Challenge, Award Recipients (1996-2009), US Environmental Protection Agency, Washington, DC, EPA 744K09002, 2009.

4. Chen, D.; Cheng, Y.; Zhou, N.; Chen, P.; Wang, Y.; Li, K.; Huo, S.; Cheng, P.; Peng, P.; Zhang, R.; Wang, L.; Liu, H.; Liu, Y.; Ruan, R. (2020). Photocatalytic degradation of organic pollutants using TiO_2-based photocatalysts: A review. *J. Clean. Prod.*, *268*, 121725.

5. Xiao, J.; Xie, Y.; Cao, H. (2015). Organic pollutants removal in wastewater by heterogeneous photocatalytic ozonation. *Chemosphere*, *121*, 1-17.

6. Ren, H.; Jin, X.; Li, C.; Li, T.; Liu, Y.; Zhou, R. (2020). Rosmarinic acid enhanced Fe(III)-mediated Fenton oxidation removal of organic pollutants at near neutral pH. *Sci. Total Environ.*, *736*, 139528.

7. Chen, J.; Xue, S.; Song, Y.; Shen, M.; Zhang, Z.; Yuan, T.; Tian, F.; Dionysiou, D.D. (2016). Microwave-induced carbon nanotubes catalytic degradation of organic pollutants in aqueous solution. *J. Hazard. Mater.*, *310*, 226-234.

8. Dai, J.R.; Liu, K.X.; Lian, F.; Tian, X.P.; Zhang, Y.F. (2023). The preparation of Co/γ-Al_2O_3 and treatment of cartap pesticide wastewater by microwave catalytic oxidation. *J. Water Process. Eng.*, *51*, 103326.

9. Cai, J.; Zhou, M.; Pan, Y.; Du, X.; Lu, X. (2019). Extremely efficient electrochemical degradation of organic pollutants with co-generation of hydroxyl and sulfate radicals on Blue-TiO_2 nanotubes anode. *Appl. Catal. B Environ.*, *257*, 117902.

10. Martínez-Huitle, C.A.; Panizza, M. (2018). Electrochemical oxidation of organic pollutants for wastewater treatment. *Curr. Opin. Electrochem.*, *11*, 62-71.

11. Dai, Y.; Zhang, N.; Xing, C.; Cui, Q.; Sun, Q. (2019). The adsorption, regeneration and engineering applications of biochar for removal organic pollutants: A review. *Chemosphere*, *223*, 12-27.

12. Awad, A.M.; Jalab, R.; Benamor, A.; Nasser, M.S.; Ba-Abbad, M.M.; El-Naas, M.; Mohammad, A.W. (2020). Adsorption of organic pollutants by nanomaterial-based adsorbents: An overview. *J. Mol. Liq.*, *301*, 112335.

13. Samanta, P.; Desai, A.V.; Let, S.; Ghosh, S.K. (2019). Advanced porous materials for sensing, capture and detoxification of organic pollutants toward water remediation. *ACS Sustain. Chem. Eng.*, *7*, 7456-7478.

14. Lv, S.W.; Liu, J.; Wang, Z.; Ma, H.; Li, C.; Zhao, N.; Wang, S. (2019). Recent advances on porous organic frameworks for the adsorptive removal of hazardous materials. *J. Environ. Sci.*, *80*, 169-185.

15. Liu, Y.; Li, W.; Gao, Y.; Wang, J.; Cheng, G.; Chen, J.; Li, X.; Zhu, G. (2022). Highly efficient and rapid removal of non-steroidal anti-inflammatory drugs from environmental samples based on an eco-friendly ZIF-67-molecularly imprinted composite. *Chem. Eng. J.*, *443*, 136396.

16. Saghir, S.; Xiao, Z. (2021). Synthesis of novel Ag@ZIF-67 rhombic dodecahedron for enhanced adsorptive removal of antibiotic and organic dye. *J. Mol. Liq.*, *328*, 115323.

17. Chen, G.; He, S.; Shi, G.; Ma, Y.; Ruan, C.; Jin, X.; Chen, Q.; Liu, X.; Dai, H.; Chen, X.; Huang, D. (2021). In-situ immobilization of ZIF-67 on wood aerogel for effective removal of tetracycline from water. *Chem. Eng. J.*, *423*, 130184.

18. Li, W.; Cao, J.; Xiong, W.; Yang, Z.; Sun, S.; Jia, M.; Xu, Z. (2020). In-situ growing of metal-organic frameworks on three-dimensional iron network as an efficient adsorbent for antibiotics removal. *Chem. Eng. J.*, *392*, 124844.

19. Chen, Q.; He, Q.; Lv, M.; Xu, Y.; Yang, H.; Liu, X.; Wei, F. (2015). Selective adsorption of cationic dyes by UiO-66-NH_2. *Appl. Surf. Sci.*, *327*, 77-85.

20. Jang, H.Y.; Kang, J.K.; Park, J.A.; Lee, S.C.; Kim, S.B. (2020). Metal-organic framework MIL-100(Fe) for dye removal in aqueous solutions: Prediction by artificial neural network and response surface methodology modelling. *Environ. Pollut.*, *267*, 115583.

21. Ahmadijokani, F.; Mohammadkhani, R.; Ahmadipouya, S.; Shokrgozar, A.; Rezakazemi, M.; Molavi, H.; Aminabhavi, T.M.; Arjmand, M. (2020). Superior chemical stability of UiO-66 metal-organic frameworks (MOFs) for selective dye adsorption. *Chem. Eng. J.*, *399*, 125346.

22. Yang, W.; Yu, T.; Sun, L.; Liu, Q.; Fei, Z.; Chen, X.; Zhang, Z.; Tang, J.; Cui, M.; Qiao, X. (2023). Pore-expanded UiO-66 pellets for efficient bisphenol A adsorption. *Chem. Eng. J.*, *455*, 140843.

23. Liu, Q.; Yao, C.; Liu, J.; Wang, S.; Shao, B.; Yao, K. (2021). An efficient method to enrich, detect and remove bisphenol A based on Fe_3O_4@MIL-100(Fe). *Microchem. J.*, *165*, 106168.

24. Yoo, D.K.; Bhadra, B.N.; Jhung, S.H. (2021). Adsorptive removal of hazardous organics from water and fuel with functionalized metal-organic frameworks: Contribution of functional groups. *J. Hazard. Mater.*, *403*, 123655.

25. Tchinsa, A.; Hossain, M.F.; Wang, T.; Zhou, Y. (2021). Removal of organic pollutants from aqueous solution using metal organic frameworks (MOFs)-based adsorbents: A review. *Chemosphere*, *284*, 131393.

26. Hasan, Z.; Choi, E.J.; Jhung, S.H. (2013). Adsorption of naproxen and clofibric acid over a meta-organic framework MIL-101 functionalized with acidic and basic groups. *Chem. Eng. J.*, *219*, 537-544.

27. Hu, T.; Jia, Q.; He, S.; Shan, S.; Su, H.; Zhi, Y.; He, L. (2017). Novel functionalized metal-organic framework MIL-101 adsorbent for capturing oxytetracycline. *J. Alloys Compd.*, *727*, 114-122.

28. Dapaah, M.F.; Liu, B.; Cheng, L. (2021). Adsorption of organic compounds from aqueous solution by pyridine-2-carboxaldehyde grafted MIL-101(Cr)-NH_2 metalorganic frameworks. *J. Environ. Chem. Eng.*, *9*, 105275.

29. Sarker, M.; Song, J.Y.; Jhung, S.H. (2018). Carboxylic-acid-functionalized UiO-66-NH_2: A promising adsorbent for both aqueous- and non-aqueous-phase adsorptions. *Chem. Eng. J.*, *331*, 124-131.

30. Lee, G.; Park, G.; Kim, S.; Jhung, S.H. (2023). Adsorptive removal of aromatic diamines from water using metal-organic frameworks functionalized with a nitro group. *J. Hazard. Mater.*, *443*, 130133.

31. Wang, C.; Kim, J.; Tang, J.; Kim, M.; Lim, H.; Malgras, V.; You, J.; Xu, Q.; Li, J.; Yamauchi, Y. (2020). New strategies for novel MOF-derived carbon materials based on nanoarchitectures. *Chem*, *6*, 19-40.

32. Ren, J.; Huang, Y.; Zhu, H.; Zhang, B.; Zhu, H.; Shen, S.; Tan, G.; Wu, F.; He, H.; Lan, S.; Xia, X.; Liu, Q. (2020). Recent progress on MOF-derived carbon materials for energy storage. *Carbon Energy*, *2*, 176-202.

33. Hao, M.; Qiu, M.; Yang, H.; Hu, B.; Wang, X. (2021). Recent advances on preparation and environmental applications of MOF-derived carbons in catalysis. *Sci. Total Environ.*, *760*, 143333.

34. Bhadra, B.N.; Yoo, D.K.; Jhung, S.H. (2020). Carbon-derived from metal-organic framework MOF-74: A remarkable adsorbent to remove a wide range of contaminants of emerging concern from water. *Appl. Surf. Sci.*, *504*, 144348.

35. Yu, F.; Bai, X.; Liang, M.; Ma, J. (2021). Recent progress on metal-organic framework-derived porous carbon and its composite for pollutant adsorption from liquid phase. *Chem. Eng. J.*, *405*, 126960.

36. Liu, D.; Gu, W.; Zhou, L.; Wang, L.; Zhang, J.; Liu, Y.; Lei, J. (2022). Recent advances in MOF-derived carbon-based nanomaterials for environmental applications in adsorption and catalytic degradation. *Chem. Eng. J.*, *427*, 131503.

37. Bhadra, B.N.; Ahmed, I.; Kim, S.; Jhung, S.H. (2017). Adsorptive removal of ibuprofen and diclofenac from water using metal-organic framework-derived porous carbon. *Chem. Eng. J.*, *314*, 50-58.

38. Yang, Y.; Ma, X.; Yang, C.; Wang, Y.; Cheng, J.; Zhao, J.; Dong, X.; Zhang, Q. (2022). Eco-friendly and acid-resistant magnetic porous carbon derived from ZIF-67 and corn stalk waste for effective removal of imidacloprid and thiamethoxam from water. *Chem. Eng. J.*, *430*, 132999.

39. Bhadra, B.N.; Song, J.Y.; Lee, S.-K.; Hwang, Y.K.; Jhung, S.H. (2018). Adsorptive removal of aromatic hydrocarbons from water over metal azolate framework-6-derived carbons. *J. Hazard. Mater.*, *344*, 1069-1077.

40. Wang, H.; Li, X.; Zhao, X.; Li, C.; Song, X.; Zhang, P.; Huo, P.; Li, X. (2022). A review on heterogeneous photocatalysis for environmental remediation: From semiconductors to modification strategies. *Chinese J. Catal.*, *43*, 178-214.

41. Zare, E.N.; Iftekhar, S.; Park, Y.; Joseph, J.; Srivastava, V.; Khan, M.A.; Makvandi, P.; Sillanpaa, M.; Varma, R.S. (2021). An overview on non-spherical semiconductors for heterogeneous photocatalytic degradation of organic water contaminants. *Chemosphere*, *280*, 130907.

42. Lacombe, S.; Keller, N. (2012). Photocatalysis: fundamentals and applications in JEP 2011. *Environ. Sci. Pollut. Res.*, *19*, 3651-3654.

43. Schneider, J.; Bahnemann, D.; Ye, J.; Li Puma, G.; Dionysiou, D.D. (2016). Photocatalysis: Fundamentals and Perspectives. Cambridge, The Royal Society of Chemistry.

44. Gopinath, K.P.; Madhav, N.V.; Krishnan, A.; Malolan, R.; Rangarajan, G. (2020). Present applications of titanium dioxide for the photocatalytic removal of pollutants from water: A review. *J. Environ. Manage.*, *270*, 110906.

45. Chen, D.; Cheng, Y.; Zhou, N.; Chen, P.; Wang, Y.; Li, K.; Huo, S.; Cheng, P.; Peng, P.; Zhang, R.; Wang, L.; Liu, H.; Liu, Y.; Ruan, R. (2020). Photocatalytic degradation of organic pollutants using TiO_2-based photocatalysts: A review. *J. Clean. Prod.*, *268*, 121725.

46. Sanakousar, F.M.; Vidyasagar, C.C.; Jiménez-Pérez, V.M.; Prakash, K. (2022). Recent progress on visible-light-driven metal and non-metal doped ZnO nanostructures for photocatalytic degradation of organic pollutants. *Mater. Sci. Semicond. Process.*, *140*, 106390.

47. Khan, S.H.; Pathak, B. (2020). Zinc oxide based photocatalytic degradation of persistent pesticides: A comprehensive review. *Environ. Nanotechnol. Monit. Manag.*, *13*, 100290.

48. Sibhatu, A.K.; Weldegebrieal, G.K.; Sagadevan, S.; Tran, N.N.; Hessel, V. (2022). Photocatalytic activity of CuO nanoparticles for organic and inorganic pollutants removal in wastewater remediation. *Chemosphere*, *300*, 134623.

49. Peleyeju, M.G.; Viljoen, E.L. (2021). WO_3-based catalysts for photocatalytic and photoelectrocatalytic removal of organic pollutants from water – A review. *J. Water Process. Eng.*, *40*, 101930.

50. Hitam, C.N.C.; Jalil, A.A. (2020). A review on exploration of Fe_2O_3 photocatalyst towards degradation of dyes and organic contaminants. *J. Environ. Manage.*, *258*, 110050.

51. Rabani, I.; Bathula, C.; Zafar, R.; Rabani, G.Z.; Hussain, S.; Patil, S.A.; Seo, Y.S. (2021). Morphologically engineered metal oxides for the enhanced removal of multiple pollutants from water with degradation mechanism. *J. Environ. Chem. Eng.*, *9*, 104852.

52. Wang, T.; Tian, B.; Han, B.; Ma, D.; Sun, M.; Hanif, A.; Xia, D.; Shang, J. (2022). Recent advances on porous materials for synergetic adsorption and photocatalysis. *Energy Environ. Mater.*, *5*, 711-730.

53. Gonçalves, J.M.; Martins, P.R.; Rocha, D.P.; Matias, T.A.; Julião, M.S.S.; Munoz, R.A.A.; Angnes, L. (2021). Recent trends and perspectives in electrochemical sensors based on MOF-derived materials. *J. Mater. Chem. C*, *9*, 8718-8745.

54. Wang, G.; Yang, S.; Cao, L.; Jin, P.; Zeng, X.; Zhang, X.; Wei, J. (2021). Engineering mesoporous semiconducting metal oxides from metal-organic frameworks for gas sensing. *Coord. Chem. Rev.*, *445*, 214086.

55. Reddy, R.C.K.; Lin, J.; Chen, Y.; Zeng, C.; Lin, X.; Cai, Y.; Su, C.-Y. (2020). Progress of nanostructured metal oxides derived from metal-organic frameworks as anode materials for lithium–ion batteries. *Coord. Chem. Rev.*, *420*, 213434.

56. Liang, P.; Zhang, C.; Sun, H.; Liu, S.; Tadé, M.; Wang, S. (2016). Photocatalysis of C, N-doped ZnO derived from ZIF-8 for dye degradation and water oxidation. *RSC Adv.*, *6*, 95903-95909.

57. Sun, L.; Shao, Q.; Zhang, Y.; Jiang, H.; Ge, S.; Lou, S.; Lin, J.; Zhang, J.; Wu, S.; Dong, M.; Guo, Z. (2020). N self-doped ZnO derived from microwave hydrothermal synthesized zeolitic imidazolate framework-8 toward enhanced photocatalytic degradation of methylene blue. *J. Colloid Interface Sci.*, *565*, 142-155.

58. Hussain, M.Z.; Schneemann, A.; Fischer, R.A.; Zhu, Y.; Xia, Y. (2018). MOF derived porous ZnO/C nanocomposites for efficient dye photodegradation. *ACS Appl. Energy Mater.*, *1*, 4695-4707.

59. Wang, Y.; Ge, S.; Cheng, W.; Hu, Z.; Shao, Q.; Wang, X.; Lin, J.; Dong, M.; Wang, J.; Guo, Z. (2020). Microwave hydrothermally synthesized framework-5 derived C-doped ZnO with enhanced photocatalytic degradation of rhodamine B. *Langmuir*, *36*, 9658-9667.

60. He, X.; Wu, M.; Ao, Z.; Lai, B.; Zhou, Y.; An, T.; Wang, S. (2021). Metal-organic frameworks derived C/TiO_2 for visible light photocatalysis: Simple synthesis and contribution of carbon species. *J. Hazard. Mater.*, *403*, 124048.

61. Li, J.; Xu, X.; Liu, X.; W. Qin, M. Wang, L. Pan (2017). Metal-organic frameworks derived cake-like anatase/rutile mixed phase TiO_2 for highly efficient photocatalysis. *J. Alloys Compd.*, *690*, 640-646.

62. Li, J.; Xu, X.; Liu, X.; Qin, W.; Pan, L. (2017). Novel cake-like N-doped anatase/rutile mixed phase TiO_2 derived from metal-organic frameworks for visible light photocatalysis. *Ceram. Int.*, *43*, 835-840.

63. Ragab; D.; Gomaa, H.G.; Sabouni, R.; Salem, M.; Ren, M.; Zhu, J. (2016). Micropollutants removal from water using microfiltration membrane modified with ZIF-8 metal organic frameworks (MOFs). *Chem. Eng. J.*, *300*, 273-279.

64. Fu, Y.-Y.; Yang, C.-X.; Yan, X.-P. (2013). Incorporation of metal-organic framework UiO-66 into porous polymer monoliths to enhance the liquid chromatographic separation of small molecules. *Chem. Commun.*, *49*, 7162-7164.

65. Prasetya, N.; Li, K. (2021). MOF-808 and its hollow fibre adsorbents for efficient diclofenac removal. *Chem. Eng. J.*, *417*, 129216.

66. Lei, Z.; Deng, Y.; Wang, C. (2018). Multiphase surface growth of hydrophobic ZIF-8 on melamine sponge for excellent oil/water separation and effective catalysis in a Knoevenagel reaction. *J. Mater. Chem. A*, *6*, 3258-3263.

67. Gao, Y.; Yan, S.; He, Y.; Fan, Y.; Zhang, L.; Ma, J., Hou, R.; Chen, L.; Chen, J. (2021). A photo-Fenton self-cleaning membrane based on NH_2-MIL-88B (Fe) and graphene oxide to improve dye removal performance. *J. Membr. Sci.*, *626*, 119192.

68. Au, A.K.; Huynh, W.; Horowitz, L.F.; Folch, A. (2016). 3D-printed microfluidics. *Angew. Chem., Int. Ed.*, *55*, 3862-3881.

69. Balakrishnan, H.K.; Doeven, E.H.; Merenda, A.; Dumée, L.F.; Guijt, R.M. (2021). 3D printing for the integration of porous materials into miniaturised fluidic devices: A review. *Anal. Chim. Acta*, *1185*, 338796.

70. Kreider, M.C.; Sefa, M.; Fedchak, J.A.; Scherschligt, J.; Bible, M.; Natarajan, B.; Klimov, N.N.; Miller, A.E.; Ahmed, Z.; Hartings, M.R. (2018). Toward 3D printed hydrogen storage materials made with ABS-MOF composites. *Polym. Adv. Technol.*, *29*, 867-873.

71. Thakkar, H.; Eastman, S.; Al-Naddaf, Q.; Rownaghi, A.A.; Rezaei, F. (2017). 3D-printed metal-organic framework monoliths for gas adsorption processes. *ACS Appl. Mater. Interfaces, 9*, 35908-35916.

72. Wu, T.; Ma, Z.; He, Y.; Wu, X.; Tang, B.; Yu, Z.; Wu, G.; Chen, S.; Bao, N. (2021). A covalent black phosphorus/metal-organic framework hetero-nanostructure for high-performance flexible supercapacitors. *Angew. Chem. Int. Ed.*, *60*, 10366-10374.

73. Lyu, Z.; Lim, G.J.H.; Guo, R.; Kou, Z.; Wang, T.; Guan, C.; Ding, J.; Chen, W.; Wang, J. (2019). 3D-Printed MOF-derived hierarchically porous frameworks for practical high-energy density Li-O_2 batteries. *Adv. Funct. Mater.*, *29*, 1-8.

74. Ying, Y.; Browne, M.P.; Pumera, M. (2020). Metal-organic-frameworks on 3D-printed electrodes: in situ electrochemical transformation towards the oxygen evolution reaction. *Sustain. Energy Fuels*, *4*, 3732-3738.

75. Liu, D.; Jiang, P.; Li, X.; Liu, J.; Zhou, L.; Wang, X.; Zhou, F. (2020). 3D printing of metal-organic frameworks decorated hierarchical porous ceramics for high-efficiency catalytic degradation. *Chem. Eng. J.*, *397*, 125392.

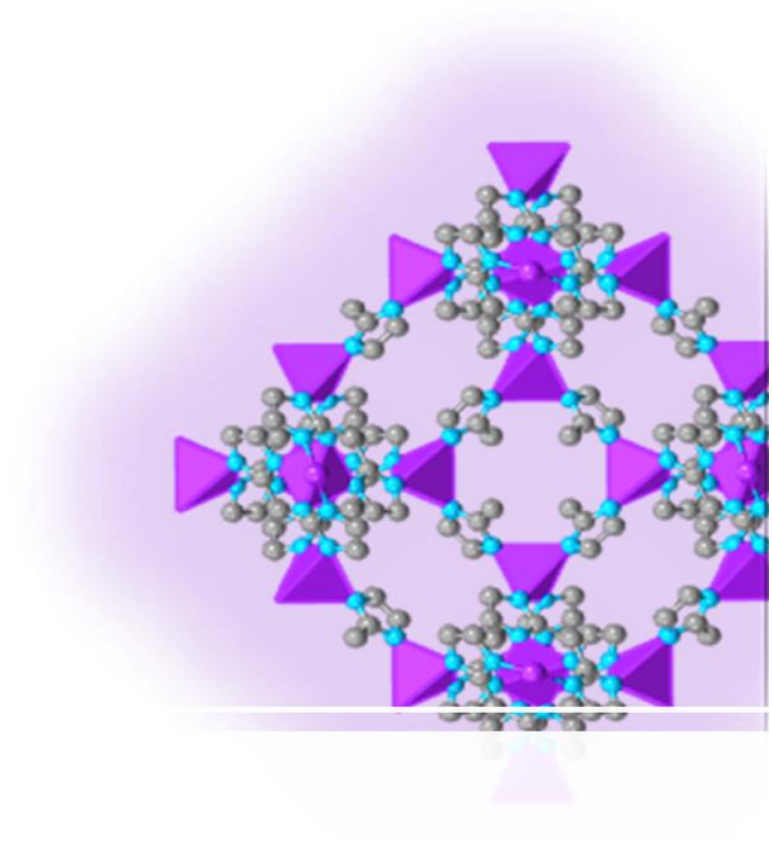

Chapter 3

Instrumental techniques

This chapter describes the fundamental principles of the different experimental techniques and instrumentation used in the characterization of the prepared MOFs and their derived materials, as well as in the monitoring of the pollutant removal processes.

Chapter 3: Instrumental techniques

3.1. Characterization techniques

Physicochemical characterization of porous materials is fundamental for understanding their properties and their behaviour. The most useful techniques in the characterization of MOFs are X-ray diffraction, nitrogen physisorption and electron microscopy, among others.

3.1.1. X-Ray diffraction

X-Ray diffraction (XRD) is a powerful non-destructive technique for the characterization of crystalline materials. It provides information about the crystalline structure and structural parameters such as average crystal size, crystallinity degree and structural defects. Fundamentally, this technique is based on the coherent scattering of an X-ray beam by matter and the constructive interference that occurs at certain angles.

In crystalline solids, the Bragg Law predicts the direction of the constructive interference between the beams by the following equation:[1,2]

$$n \cdot \lambda = 2 \cdot d_{hkl} \cdot sin\ \theta_{hkl} \quad \text{[Equation 1]}$$

where ***n*** is the diffraction order, ***λ*** is the wavelength of the incident radiation, ***d*** is the interplane distance, ***θ*** is the diffraction angle and ***hkl*** are the Miller indices of the chosen diffraction line.

From the diffractogram it is possible to determine the diffraction angles and, with the wavelength and using *equation 1,* the interplane distances can be calculated. With the ***d*** values, it is also possible to assign the indices to the different reflections, which allows to determine the crystal symmetry and even the crystal lattice parameters (the angles and dimensions of the unit cell).

The XRD pattern is unique to each compound. Therefore, this technique allows us to: (i) identify solids by comparing the obtained diffractogram with those found in the bibliography and (ii) determine the crystal purity of the sample.[3]

Experimental method

The materials studied in this work were characterized by a *Bruker D8 Advance* X-ray diffractometer equipped with a copper anticathode (CuK_α radiation), a nickel filter and a Lynxeye one-dimensional energy dispersive detector. The Bragg-Brentano geometry of the instrument and its schema of operation is shown in the *Figure 3.1*.

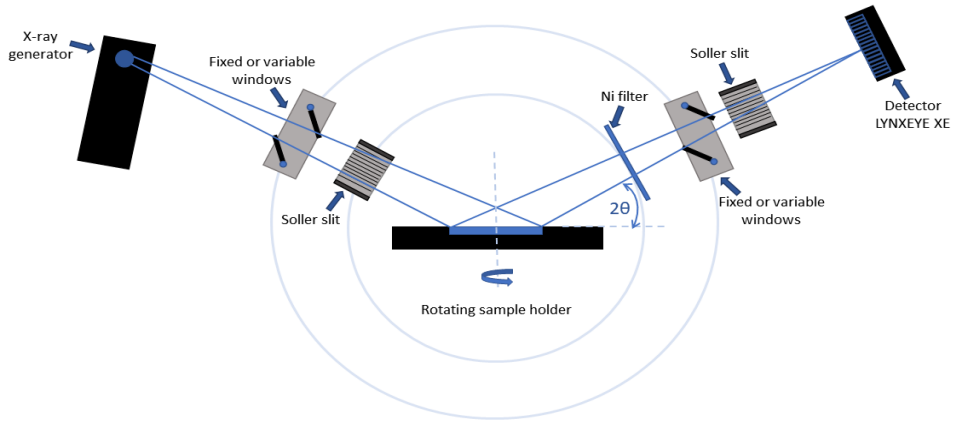

Figure 3.1. Bragg-Brentano geometry of the diffractometer.

The radiation from the X-ray tube is diffracted by the sample and collected by the one-dimensional energy dispersive detector. The detector has a system of fixed or variable windows through which it is delimited the lighting area of the sample and eliminated unwanted scattered radiation. It also has two Soller slits formed by a set of parallels metal sheets that limit the vertical divergence of the X-ray beam and, finally, before reaching the detector, the diffractometer includes a nickel filter to remove the K_β component from the radiation.

The diffraction measurements were performed in air and at room temperature. *Table 3.1* specifies the experimental conditions used.

Table 3.1. Experimental conditions used to obtain diffractograms.

Radiation	CuK_α (λ=1.5418 Å)
Angular interval (2θ)	1.5-35º or 5-75º
Step size	0.01º, 2θ
Residence time	1 second/step
Voltage	40 kV
Intensity	40 mA
Opening of the divergence slits	0.68 mm

3.1.2. N_2 adsorption-desorption

There are several different techniques to carry out the textural characterization of materials, being the physical adsorption of gases one of the most used.[4,5] The processes of gas adsorption on the surface of a solid are divided into two categories depending on the type of adsorbate-adsorbent interactions: physisorption (physical reversible interaction) and chemisorption (chemical interactions, non-reversible). Physisorption has a series of characteristics that make it particularly suitable for the textural analysis of materials:[6] (i) it involves only dispersive forces, so the adsorption heats are low, in the order of latent heat of vaporization or sublimation of the adsorbate, (ii) the adsorption is reversible and nonspecific, allowing the study of the adsorption and desorption phenomena and (iii) it can be extended beyond the monolayer producing a multilayer adsorption.

For a given gas/solid system, the amount of gas adsorbed per gram of solid, ***x***, at constant temperature, ***T***, depends on the pressure ***p*** by the following equation:

$$x = f(p)T \quad \text{[Equation 2]}$$

If the temperature is below the critical temperature of the adsorbate, it behaves like a vapor. In this case, it is convenient to replace the absolute pressure ***p*** by the relative pressure $\boldsymbol{p/p_0}$, where $\boldsymbol{p_0}$ is the saturation pressure of the gas at the measurement temperature, ***T***. Accordingly, Equation 2 can be written as:

$$x = f\left(\frac{p}{p_0}\right)T \quad \text{[Equation 3]}$$

The graphical representation of the amount of gas adsorbed, ***x***, as a function of relative pressure, $\boldsymbol{p/p_0}$, at constant temperature, ***T***, is known as the adsorption isotherm. The type of the isotherm depends on the type of pores of the solid and the relative values of the adsorbate-adsorbent interaction energies. According to the IUPAC classification, most adsorption isotherms can be grouped into one of the six types represented in the *Figure 3.2*. The first five isotherms, Types I to V, appeared in the initial classification proposed by *Brunauer, Deming, Deming, and Teller* (BDDT classification).[5] Isotherm VI was identified later.[7]

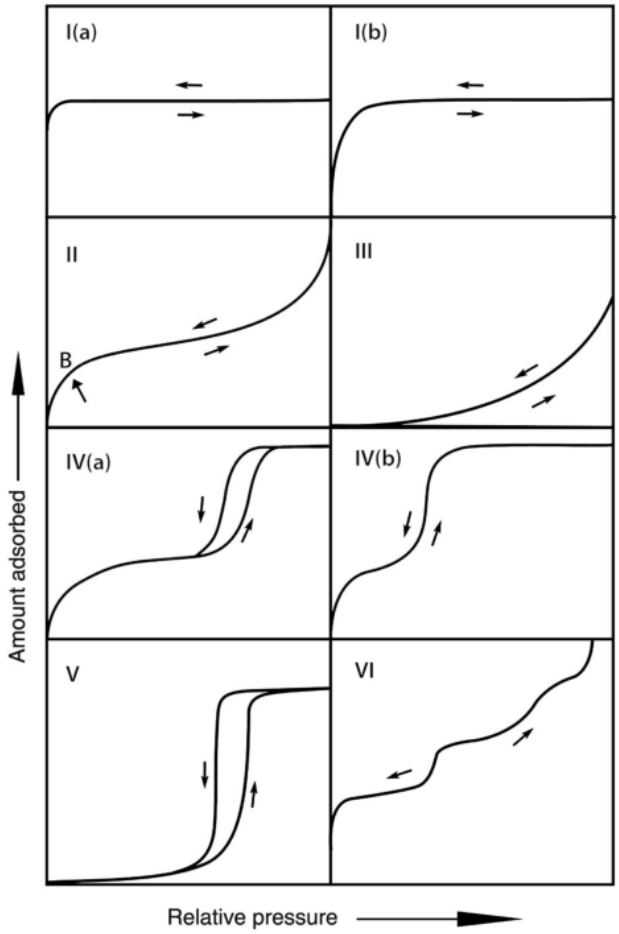

Figure 3.2. Classification of physisorption isotherms.

Reversible Type I isotherms are characteristic of microporous solids (some activated carbons, molecular sieve zeolites and certain porous oxides) having relatively small external surfaces. The high adsorption energy allows the gas to be adsorbed at low pressures. For nitrogen adsorption at 77 K, Type I(a) isotherms are presented by microporous materials with mainly narrow micropores (of width <~1 nm); while Type I(b) isotherms are typical of materials with larger pore sizes, around 2.5 nm.

Reversible Type II and Type III isotherms are characteristic of gas physisorption on nonporous or macroporous adsorbents. The shape is the result of unrestricted monolayer-multilayer adsorption up to a relative pressure close to 1. The point B generally corresponds to the end of the monolayer coverage. In Type III isotherm, there is no Point B and therefore no identifiable monolayer formation.

Type IV isotherms are given by mesoporous adsorbents, such as many oxide gels, industrial adsorbents, and mesoporous molecular sieves. The adsorption behaviour in mesopores is determined by the adsorbent-adsorbate interactions and by the interactions

between the molecules in the condensed state. In the case of a Type IV(a) isotherm, capillary condensation is accompanied by hysteresis. This phenomenon occurs when the pore width exceeds a certain critical width, that depends on adsorption system and process temperature. Type IV(b) isotherms are given by conical and cylindrical mesopores.

Reversible type V isotherms are also characteristic of mesoporous materials. In the low p/p_0 range, the shape of the isotherm Type V is very similar to that of Type III, and this can be attributed to relatively weak adsorbent-adsorbate interactions. At higher p/p_0, these interactions are followed by pore filling.

The reversible stepwise Type VI isotherm is representative of layer-by-layer adsorption on a highly uniform nonporous surface.

Frequently, adsorption-desorption isotherms present a zone of partially irreversibility in which the retention of a certain amount of gas takes place at a relatively higher-pressure during adsorption than at desorption, forming a loop or hysteresis cycle. Reproducible, permanent hysteresis loops, which are in the multilayer range of physisorption isotherms, are generally associated with capillary condensation. Hysteresis cycles can adopt many forms, each of which corresponds to a certain geometry and pore size. *Figure 3.3* shows the classification of the type of hysteresis cycles according to IUPAC.[7]

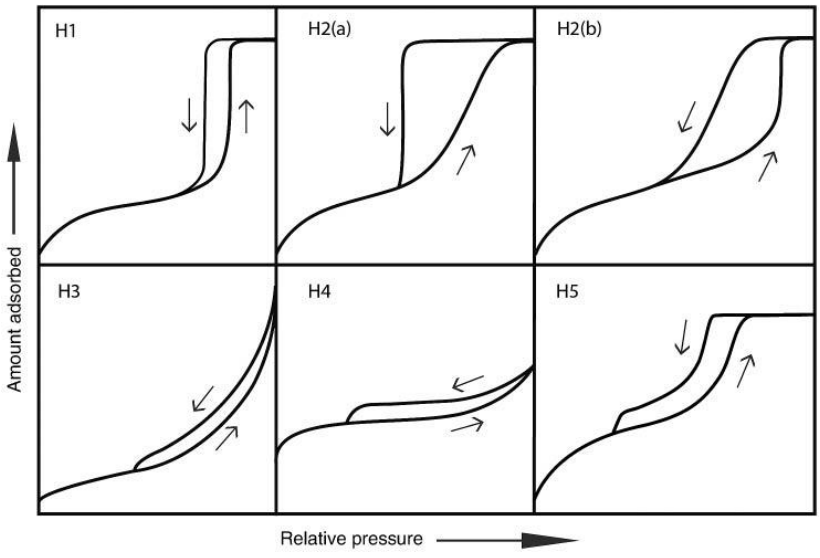

Figure 3.3. Classification of hysteresis loops.

The determination of the specific surface area of a solid from its adsorption isotherms requires knowledge of: (i) the monolayer capacity, ***Xm***, which is the amount of adsorbate per gram of solid needed to get the surface completely covered by a monolayer and (ii) the surface

covered by an adsorbate molecule, ***Am***, which, in the case of nitrogen at 77 K, is considered 16.2 Å.[8]

The relation between the surface area and these magnitudes is:

$$s(m^2/g) = \frac{X_m \cdot N \cdot A_m \cdot 10^{-20}}{M} \quad \text{[Equation 4]}$$

where ***N*** is the Avogadro's number, ***M*** is the molecular weight of the adsorbate and 10^{-20} is a necessary factor for the conversion of $Å^2$ to m^2.

The determination of the specific surface area of a material requires knowing the monolayer capacity, which can be obtained from the adsorption isotherm by application of simplified mathematical methods. Despite the oversimplification of the model applied, the *Brunauer-Emmett-Teller* (BET) method has become the most widely used standard procedure for determining the specific surface area of finely divided and porous materials.[9] The model is an extension of Langmuir adsorption treatment.

The BET equation is usually used in its linear form:

$$\frac{p}{V_{ads} \cdot (p_0 - p)} = \frac{1}{V_m \cdot C} + \left(\frac{C-1}{V_m \cdot C}\right) \cdot \frac{p}{p_0} \quad \text{[Equation 5]}$$

where $\boldsymbol{V_{ads}}$ is the amount of adsorbed gas per gram of adsorbate at relative pressure $\boldsymbol{p/p_0}$, $\boldsymbol{V_m}$ is the monolayer capacity expressed in cm^3 of adsorbent per gram of adsorbate and ***C*** is a constant related to the heat enthalpy of the first layer adsorption. Although the value of ***C*** can be used to characterize the shape of the isotherm, it does not provide a quantitative measure of the adsorption enthalpy. It only provides a simple indication of the magnitude of the interaction energy between adsorbate and adsorbent.

Plotting $\boldsymbol{p/[V_{ads}(p_0-p)]}$ versus $\boldsymbol{p/p_0}$, a linear correlation is obtained in the low-pressure zone, usually with $\boldsymbol{p/p_0}$ between 0.05 and 0.3, which corresponds to the pressure range in which the BET equation correctly describes the isotherm. From the slope and the Y-intercept, obtained by adjusting the line by the least squares method, the monolayer capacity, $\boldsymbol{V_m}$, and the ***C*** value are determined. The monolayer capacity in cm^3 can be converted to the corresponding value of $\boldsymbol{X_m}$, and once obtained, the specific surface area can be determined using *Equation 4.*

On the other hand, the *Two-Dimensional Non-Local Density Functional Theory* (2D-NLDFT),[10] is one of the most used methods for the determination of pore distribution. This method is applied to calculate the properties of the condensed sorptive fluid within the pore, generating theoretical isotherms that indicate the amount of gas adsorbed as a function of pore

size and pressure at specific conditions. Applying a mathematical comparison between these theoretical isotherms with the experimental ones, the pore size of the samples is obtained.

Experimental method

The experimental determination of the adsorption-desorption isotherms presented in this thesis was performed with an automated instrument, *Micromeritics Tristar II 3020 analyser*, using nitrogen as an adsorbate and helium to calibrate the dead volumes that cannot be measured. Before nitrogen adsorption, the sample was previously degassed at 140 or 200 °C for 12 hours.

3.1.3. Electron microscopy

Morphological characterization of the materials was carried out by scanning electron microscopy (SEM) and transmission electron microscopy (TEM).

When a high-energy electron beam impacts upon matter, a series of signals are produced, and the detection and quantification of them is the basis of the different electron microscopy techniques.[11] One of the possibilities is that the primary electrons (electrons of the beam) collide with the more external electrons of the sample, knocking them off. These secondary electrons are the basis of the scanning electron microscopy. On the other hand, the primary electrons can also interact with the more internal electrons of the sample, exciting them. During the relaxation process, these electrons emit characteristic X-radiation that provides information about the chemical composition of the sample (EDS, *Energy dispersive X-Ray Analysis*).[12] Besides, depending on the thickness and the composition of the sample, when the electron beam impacts, the electrons of the sample can be transmitted or elastically scattered (diffracted). These transmitted electrons are used by transmission electron microscopy for obtaining images.

With SEM it is possible to know the morphology and the crystal size of a solid.[13] For this reason, it is a very useful technique for the set-up of synthesis methods. The SEM has a large depth of field, which allows to simultaneously focus areas at different heights of the sample and to produce an image that is a good representation of the three-dimensional sample. So, using this technique, it is possible to obtain images with high definition and resolution, as long as the

particle size is at least 60 nm. Below that value, it is necessary to use transmission electron microscopy, which offers a two-dimensional image of the solid. In this case, in order to minimize the interactions of the beam with the sample atoms, it is necessary to use very thin samples so the electron beam can pass through them.

The path of the electron beams in SEM and TEM microscopes are represented in *Figure 3.4* and *Figure 3.5*, respectively.

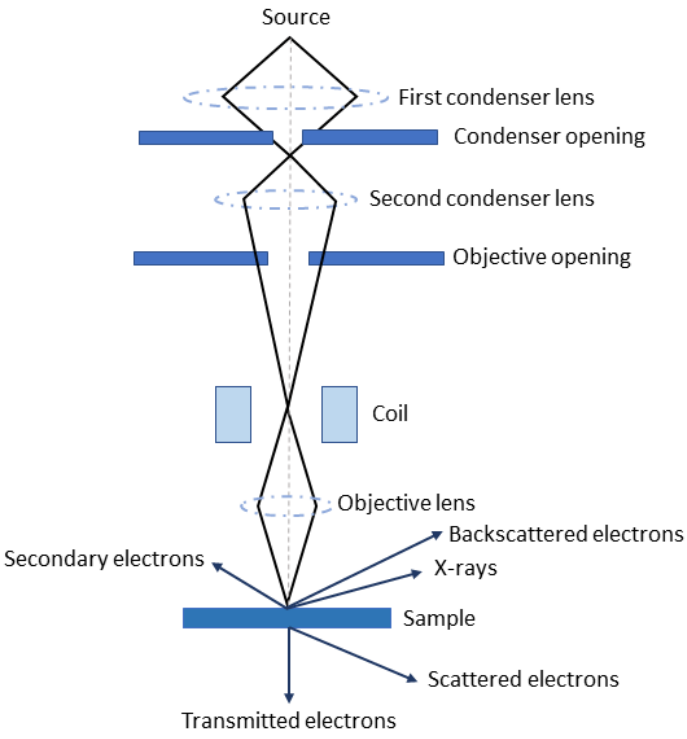

Figure 3.4. Scanning electron microscope diagram.

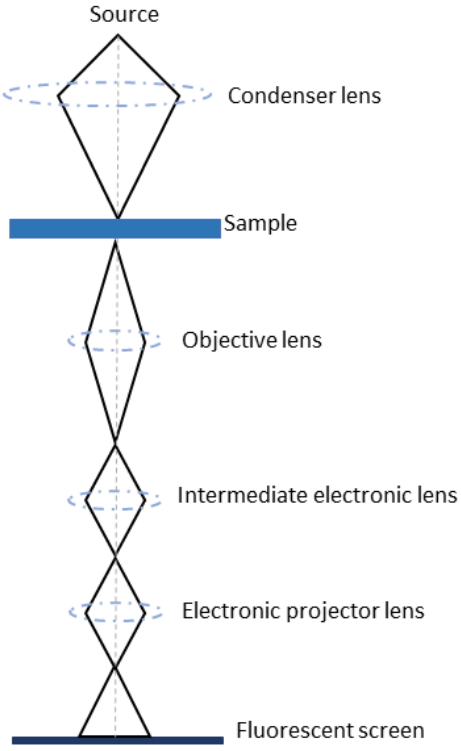

Figure 3.5. Transmission electron microscope diagram.

Experimental method

The SEM images presented in this thesis were obtained with a *Hitachi S-3400N* scanning electron microscope, operating at 15 kV. To avoid problems caused by the accumulation of electrical charge, the samples were coated by vaporization with a thin layer of gold. EDAX analysis was performed using a *Bruker AXS XFlash 4010* EDAX detector coupled to the scanning electron microscope.

To obtain the TEM images, a *Hitachi H-600 ABS* TEM was used, operating at 100 kV, whose maximum resolution is 4.5 Å. For the analysis, the samples were dispersed in pure ethanol and spotted on a copper grid. The dried samples were analysed under a high vacuum.

3.1.4. Thermogravimetric analysis

Thermogravimetry is an analysis technique that records the mass loss of a solid as a function of temperature. Among the various existing modalities, the most used is dynamic thermogravimetry. In this modality, the mass of the sample is continuously recorded as the temperature increases linearly.[14]

The representation of the mass change versus the temperature, or thermogram, provides information about the thermal stability of the sample, the presence of adsorbed molecules on the surface and about the composition of the initial sample and the residue.

Experimental method

The thermograms presented in this thesis have been used to determine the mass of residue obtained after heating each of the studied samples. They were registered using a *SDT 2960* (TA Instruments) equipped with a DSC-TGA simultaneous analyser (*Figure 3.6*). The samples were heated in air from 25 °C to 800 °C, using a heating rate of 5 °C/min.

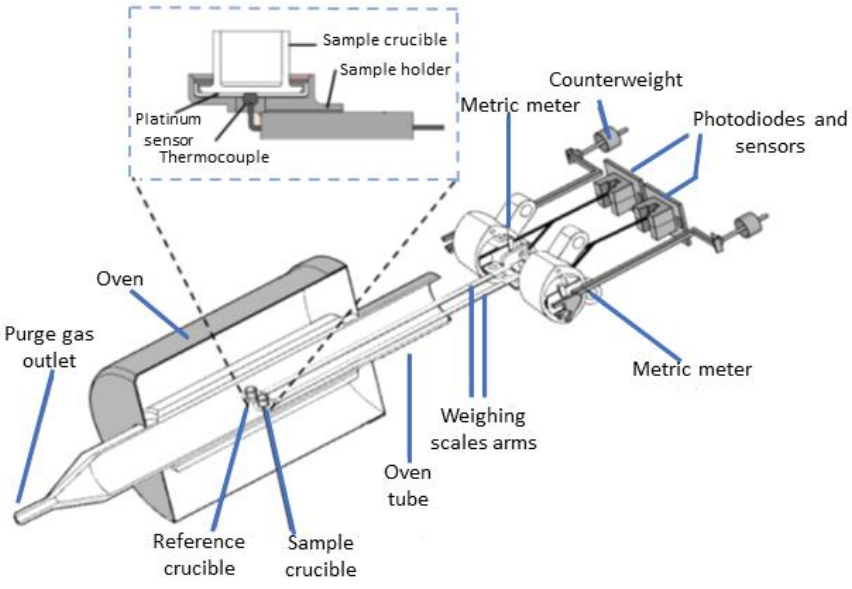

Figure 3.6. SDT 2960 thermobalance diagram.

3.1.5. Zeta Potential

Zeta potential is used in colloidal chemistry to study the behaviour of dispersive systems in liquids. It is also used to characterize the electrical double layer at the solid-liquid interface.

In contact with a polar environment as water, the surface of the particles is charged because of ionization processes, physical adsorption and ionic solution. This superficial charge affects the arrangement of the ions in the polar environment. Oppositely charged ions are attracted to the surface of the particle and ions of the same sign are repelled.[15]

An electrical double layer is formed because of thermal or Brownian motion.[16,17] This double layer consists of a charged surface and oppositely charged ions, which are diffusely distributed throughout the polar medium. The existence of the electrical double layer is related to the electrostatic interaction between the particles in suspension and, consequently, to the stability of the suspension.

Accordingly, the zeta potential depends on many factors such as solvent composition, chemical composition of the particle's surface, pH, and suspended ions.

Experimental method

The zeta potential measurements were carried out by microelectrophoresis technique. This technique uses two electrodes connected at the edges of a chamber, which, when connected to a power source, create an electric field that crosses the cell. Charged colloids move within the electric field and their direction is related to the zeta potential (*Figure 3.7*).

A *Malvern Zetasizer Nano ZS90* instrument was used to carry out the zeta potential measurements in this doctoral thesis. The isoelectric point of the prepared materials was determined by plotting the zeta potential against pH.

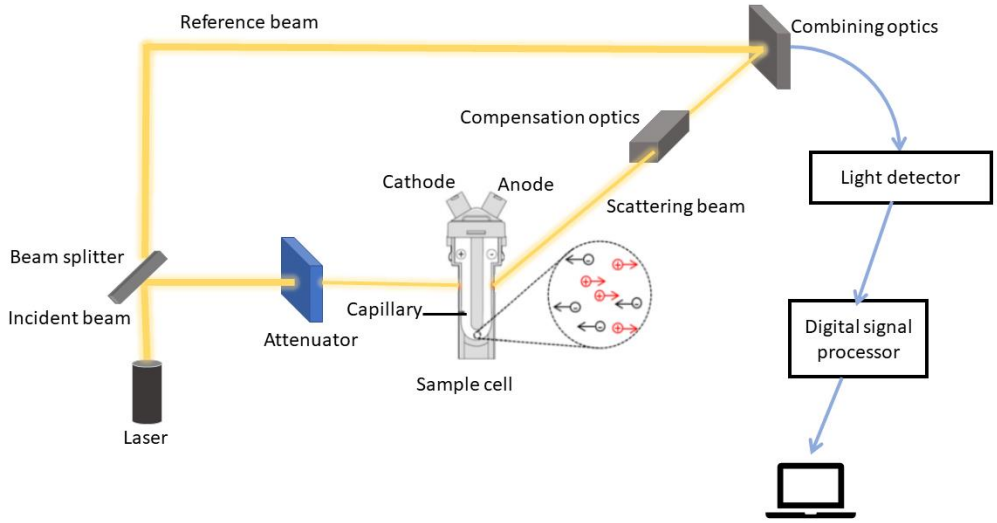

Figure 3.7. Malvern Zetasizer Nano ZS90 diagram.

3.1.6. FTIR spectroscopy of probe molecules

Infrared spectroscopy of probe molecules is a very useful technique for the study of the surface, both internal and external, of porous solids as metal-organic frameworks.[18-20] This technique is based on the adsorption of molecules on the surface of a solid and in the study of the modifications produced to the IR spectra due to adsorbate-adsorbent interaction.

As a result of this interaction, the most significant changes in the vibrational spectra of the adsorbed molecules are: (i) variation of active modes due to a change in the symmetry and (ii) changes in the wavenumber and also in the intensity and width of the characteristic IR absorption bands. In addition, when the molecular probe interacts with the porous solid, the vibrations of the framework and of the hydroxyl groups present on the surface of the solid are also usually modified. The study of these modifications, both, those of the molecular probe and those of the adsorbent, allows to obtain information on: (i) Brønsted acidity that is given by the surface hydroxyl groups, (ii) Lewis acidity, due to the presence of coordinatively unsaturated metal sites, (iii) oxidation state and environment of the metal centers and (iv) functional groups present in the framework.

In IR spectroscopy, the choice of the molecular probe is very important. The selection depends on the system under study, but in general, the molecule used as a spectroscopic probe should have certain properties:

(i) Its interaction with the surface of the solid should create a spectroscopic response that can be easily detected. This response must be able to discriminate between active centers of different nature (oxidation states). The probe molecule must be also sensitive to the environment of the metal centers.

(ii) The molar absorption coefficients of the characteristic vibration modes of the probe must be high, to ensure optimal sensitivity. If quantitative studies are also carried out, their values must be known.

(iii) The shift of the IR absorption band produced due to the interaction between the probe and the solid surface must be measurable with precision. Therefore, these shifts must be greater than the intrinsic bandwidth of the considered vibration modes.

(iv) The interaction of the probe molecule with the solid, at the working temperature and pressure conditions, must be weak enough to avoid chemical reaction with the porous material.

The most common molecules used as spectroscopic probes, such as CO, CO_2, N_2, H_2, CD_3CN, pyridine, ... have relatively simple structures and present bands in the infrared spectrum that are easily distinguishable from those resulting from the solid under study. However, it is often difficult to find a single molecule that satisfactorily meets the requirements for fully characterizing a material, therefore two or more different probes are often used.

The small size of CO (kinetic diameter of 0.376 nm) makes this molecule a good candidate for the study of the surface of metal-organic frameworks. For this reason, it has been used in the characterization of these and other solids.[20-23]

The interaction of CO with the solid acid centers gives rise to the appearance of, in the C–O stretching region of the IR spectrum, as many bands as the number of different acid centers recognize the molecule. The CO interacts, through the carbon atom, with the acid centers of the solid, forming OH···CO and M^{n+}···CO adducts with the Brønsted and Lewis acid centers, respectively.[24,25] Due to the polarization induced in the CO by the interaction of the molecule with the acid centers, there is an increase in the vibration wavelength with respect to the free molecule. The magnitude of this hypsochromic shift is a measure of the acid center strength: the greater the shift, the greater the acid strength. CO can also interact through the oxygen atom with the acid centers of the solid, forming adducts OH···OC and M^{n+}···OC with Brønsted and Lewis acid centers, respectively.[26,27] In this case, as a consequence of the interaction, the vibration

wavelength of CO decreases, and the magnitude of the bathochromic shift is also a measure of the acid strength of the center.

Experimental method

The IR spectra of adsorbed carbon monoxide presented in this thesis were obtained using a quartz cell with sodium chloride windows and a central tube, consisting of a copper sample holder, which allows to cool the sample with liquid nitrogen (*Figure 3.8*). The samples were prepared as thin self-supported wafers and thermally activated (180 ^{o}C during 8 h) under dynamic vacuum before the analysis. Once the activation process was finished, the cell was transferred to the measurement cavity of a *Bruker Vertex 80v* spectrophotometer, working at 3 cm^{-1} resolution, and the infrared spectra were acquired before and after CO adsorption.

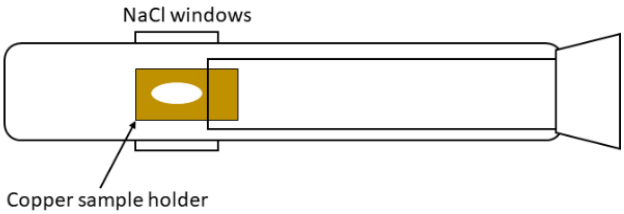

Figure 3.8. Quartz cell for carrying out IR spectroscopy experiments using CO as molecular probe.

3.1.7. UV-Vis diffuse reflectance spectroscopy (DRS)

UV-Vis spectroscopy is a technique that provides information about the electrical structure of materials and their optical properties.

When a semiconductor solid is exposed to a radiation of adequate wavelength, it produces electronic transitions from the valence band to the conductive band of the solid, resulting in the apparition of an absorption band in the UV-Vis spectrum. The fundamental transition between the semiconductor bands, makes it possible to calculate the band gap (***Eg***), using the Kubelka-Munk equation:[28]

$$(F(R)\cdot hv)^n = (hv - Eg) \quad \text{[Equation 6]}$$

where ***Eg*** is the band gap energy, $\boldsymbol{hv}$ corresponds to the energy of the incident photon, ***n*** can take values of ½ or 2 depending on the type of transition (direct or indirect), and ***F(R)*** is proportional to the extinction coefficient and is described by the following equation:

$$F(R) = \frac{(1-R)^2}{2R}$$ [Equation 7]

where ***R*** is the diffuse reflectance in %.

Then, plotting ***[F(R)·hν]^n*** against the photon energy (***hν***), a curve is obtained. By applying linear regression to the part with greater slope and by extrapolating this line to a value of F(R) = 0, the value of ***hν*** corresponds to the band energy (***Eg***) according to Equation 6.

Experimental method

UV-Vis diffuse reflectance was used for the determination of the band gap of the prepared titanium oxides derived from the NTU-9 metal organic framework. This measurement was carried out with a *Thermo-Fisher Scientific Evolution 300* spectrometer, equipped with a diffuse reflectance accessory (integration sphere).

3.2. Analytical techniques

3.2.1. Ultraviolet-visible spectroscopy

The ultraviolet-visible spectrum (UV-Vis) originates from the electronic transitions of molecules.[29] This technique is frequently used in the quantitative determination of the concentration of absorbent species in solution through the Lambert-Beer law, which establishes that the absorbance, ***A***, is proportional to the concentration of the absorbent species, ***c***, according to the equation:[29-31]

$$A = \varepsilon\, l\, c$$ [Equation 8]

where $\boldsymbol{\varepsilon}$ is the molar absorption coefficient (characteristic of each substance) and $\boldsymbol{l}$ is the optical path.

Experimentally, the sample is irradiated with UV-Vis electromagnetic radiation of wavelength between 200 and 800 nm. The transmitted light is recorded by a detector located on the opposite side. *Figure 3.9* represents a double beam UV-Vis spectrophotometer.

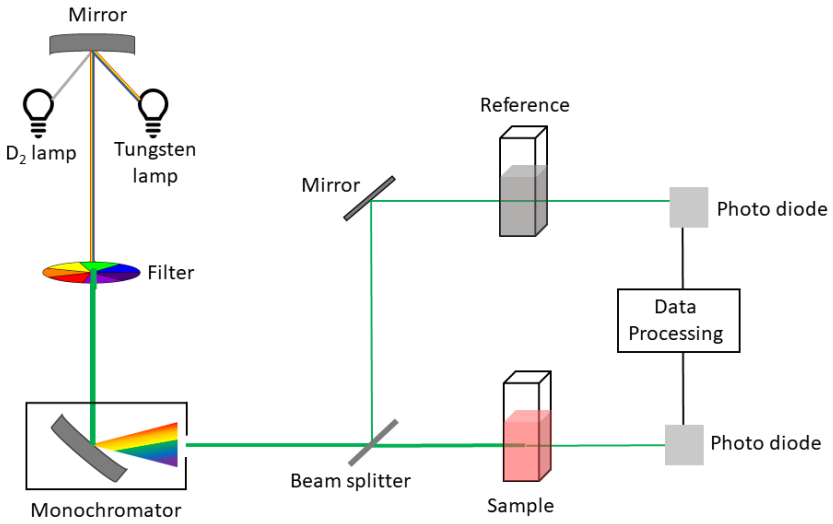

Figure 3.9. Diagram of a double-beam UV-Vis spectrophotometer. The tungsten lamp emits visible light, and the deuterium lamp emits ultraviolet light.

Experimental method

In this work, UV-Vis spectroscopy was used to quantify the adsorption or degradation of various organic pollutants. The spectroscopic measurements were carried out with a *Jasco V-730* UV-Vis spectrophotometer.

3.2.2. High performance liquid chromatography (HPLC)

High performance liquid chromatography is a very popular analytical technique used for the separation, identification and quantification of substances present in a mixture.[32]

It is an advanced chromatography technique that uses pumps to pass a pressurized liquid solvent containing a mixture of the analytes through a column filled with a solid adsorbent material (the stationary phase). The adsorbent is a granular material (silica, polymers, ...) composed of solid particles of size between 2 and 50 µm. The pressurized fluid (the mobile phase) is normally composed of a solvent mixture (water, acetonitrile, methanol, among others). When a small volume of the sample (typically microliters) is introduced into the stream of the mobile phase, each component in the sample interacts slightly differently with the stationary phase, causing different flow rates for the different components and leading to their separation as they flow out of the column. The retention of the components depends on the nature of the compound and the composition of both the stationary and the mobile phase. The time at which

a specific analyte elutes from the column is called its retention time. The retention time, measured under specific conditions, is characteristic of each analyte, allowing their identification. *Figure 3.10* shows a diagram of the HPLC equipment.

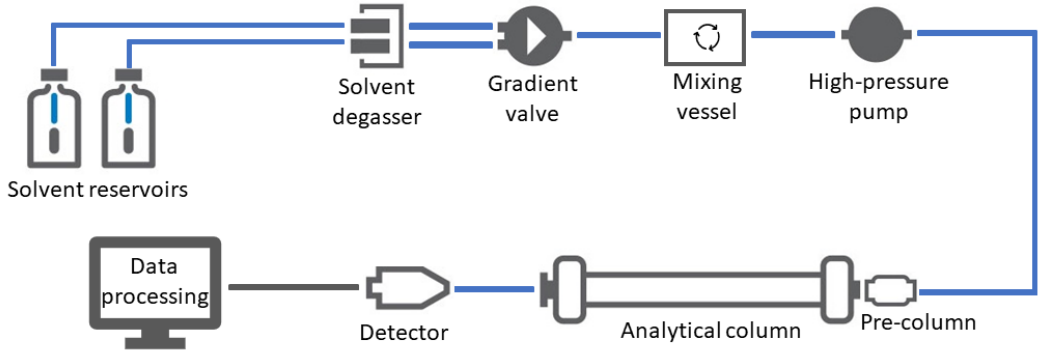

Figure 3.10. Diagram of the HPLC equipment.

HPLC differs from traditional liquid chromatography in that its operational pressures are significantly higher (50-350 bar). There are many types of HPLC techniques, depending on the interaction between the sample and both phases, such as partition chromatography, normal-phase chromatography, reversed-phase chromatography, size-exclusion chromatography, ion-exchange chromatography, and bioaffinity chromatography. Moreover, the HPLC uses different types of detectors to generate a processing signal, the most common being UV/Vis, photodiode array (PDA) or mass spectrometry.

Experimental method

The reversed-phase HPLC was used for the separation and determination of different pharmaceuticals and phenols from a mixture. The stationary phase was composed of silica particles (*C18 SpeedCore* column), and the mobile phase was a mixture of acetonitrile-water. The instrument used was a *HPLC Jasco* Chromatograph equipped with a high-pressure pump (*PU-4180*), a manual injector, and a photo diode matrix (*MD-4017*).

3.3. Bibliographic references

1. James, R.W. (1962). The Optical Principles of the Diffractions on X-Rays. *London, G. Bells and Sons.*

2. Bragg, W.H. (1915). The structure of magnetite and spinels. *Nature*, *95*, 561.

3. Kohli, R.; Mittal, K.L. (2019). Developments in surface contamination and cleaning. Vol. 12, pp. 23-105, *Elsevier*.

4. Sing, K.S.; Everett, D.H.; Haul, R.A.W.; Moscou, L.; Pierotti, A.; Rouquerol, J.; Siemieniewska, T. (1985). Reporting physisorption data for gas/solid systems with special reference to the determination of surface area and porosity. *Pure Appl. Chem.*, *57*, 603-619.

5. Brunauer, S.; Deming, L.S.; Deming, W.E.; Teller, E. (1940). Theory of the Van der Waals adsorption of gases. *J. Am. Chem. Soc.*, *62*, 1723-1732.

6. Agboola, O.D.; Benson, N.U. (2021). Physisorption and chemisorption mechanisms influencing micro (nano) plastics-organic chemical contaminants interactions: A Review. *Front. Environ. Sci.*, *9*, 678574.

7. Thommes, M.; Kaneko, K.; Neimark, A.V.; Olivier, J.P.; Rodriguez-Reinoso, F.; Rouquerol, J.; Sing, K.S.W. (2015). Physisorption of gases, with special reference to the evaluation of surface area and pore size distribution (IUPAC Technical Report). *Pure Appl. Chem.*, *87*, 1051-1069.

8. Brunauer, S.; Emmet, P.; Teller, E. (1938). Adsorption of gases in multimolecular layers. *J. Am. Chem. Soc.*, *60*, 309-319.

9. Emmett, P.H.; Brunauer, S. (1937). The use of low temperature van der Waals adsorption isotherms in determining the surface area of iron synthetic ammonia catalysts. *J. Am. Chem. Soc.*, *59*, 1553-1564.

10. Jagiello, J.; Olivier, J.P. (2013). 2D-NLDFT adsorption models for carbon slit-shaped pores with surface energetical heterogeneity and geometrical corrugation. *Carbon*, *55*, 70-80.

11. Vernon-Parry, K.D. (2000). Scanning electron microscopy: an introduction. *III-Vs Review*, *13*, 40-44.

12. Scimeca, M.; Bischetti, S.; Lamsira, H.K.; Bonfiglio, R.; Bonanno, E. (2018). Energy Dispersive X-ray (EDX) microanalysis: A powerful tool in biomedical research and diagnosis. *Eur. J. Histochem.*, *62*, 89-99.

13. Stokes, D. (2022). Principles and Practice of Variable Pressure: Environmental Scanning Electron Microscopy (VP-ESEM). *Wiley.*

14. Lothenbach, B.; Durdzinski, P.; De Weerdt, K. (2016). Thermogravimetric analysis. A Practical Guide to Microstructural Analysis of Cementitious Materials*. CRCPress.*

15. Bhattacharjee, S. (2016). DLS and zeta potential - What they are and what they are not? *J. Controlled Release*, *235*, 337-351.

16. Hunter, R.H. (1981). Zeta potential in colloids science. Principles and application. *School of Chemistry, University of Sydney (Australia). Academic Press.*

17. Liao, D.L.; Wub, G.S.; Liao, B.Q. (2009). Zeta potential of shape-controlled TiO_2 nanoparticles with surfactants. *Colloids Surf. A: Physicochem. Eng. Asp.*, *348*, 270-275.

18. Volkringer C.; Leclerc H.; Lavalley, J.C.; Loiseau, T.; Férey, G.; Daturi, M.; Vimont, A. (2012). Infrared spectroscopy investigation of the acid sites in the metal-organic framework aluminum trimesate MIL-100(Al). *J. Phys. Chem. C*, *116*, 5710-5719.

19. Valenzano, L.; Civalleri, B.; Chavan, S.; Palomino, G.T.; Areán, C.O.; Bordiga, S. (2010). Computational and experimental studies on the adsorption of CO, N_2, and CO_2 on Mg-MOF-74. *J. Phys. Chem. C.*, *114*, 11185-11191.

20. Wang, J.; Wang, W.; Fan, Z.; Chen, S.; Nefedov, A.; Heißler, S.; Fischer, R.A. Wöll, C.; Wang, Y. (2021). Defect-engineered metal-organic frameworks: A thorough characterization of active sites using CO as a probe molecule. J. Phys. Chem. C, *125*, 593-601.

21. Jodłowski, P.J.; Kurowski, G.; Dymek, K.; Jędrzejczyk, R.J.; Jeleń, P.; Kuterasiński, Ł.; Gancarczyk, A.; Węgrzynowicz, A.; Sawoszczuk, T.; Sitarz, M. (2020). In situ deposition of M(M=Zn; Ni; Co)-MOF-74 over structured carriers for cyclohexene oxidation - Spectroscopic and microscopic characterisation. *Microporous Mesoporous Mater.*, *303*, 110249.

22. Lansford, J.L.; Vlachos, D.G. (2020). Infrared spectroscopy data- and physics-driven machine learning for characterizing surface microstructure of complex materials. *Nat. Commun.*, *11*, 1513.

23. Noei, H.; Kozachuk, O.; Amirjalayer, S.; Bureekaew, S.; Kauer, M.; Schmid, R.; Marler, B.; Muhler, M.; Fischer, R.A.; Wang, Y. (2013). CO Adsorption on a mixed-valence ruthenium metal-organic framework studied by UHV-FTIR spectroscopy and DFT Calculations. *J. Phys. Chem. C*, *117*, 5658-5666.

24. Scarano, D.; Spoto, G.; Zecchina, A.; Reller, A. (1989). Relations between the morphology of ZnO microcrystals and their adsorptive properties towards CO as studied by IR spectroscopy. *Surf. Sci.*, *211*, 1012-1017.

25. Dixon, D.A.; Gole, J.L.; Komornicki, A. (1988). Lithium and sodium cation affinities of H_2, N_2, and CO. *J. Phys. Chem.*, *92*, 1378-1382.

26. Bordiga, S.; Palomino, G.T.; Pazè, C.; Zecchina, A. (2000). Vibrational spectroscopy of H_2, N_2, CO and NO adsorbed-on H, Li, Na, K-exchanged ferrierite. *Microporous Mesoporous Mater.*, *34*, 67-80.

27. Bordiga, S.; Lamberti, C.; Geobaldo, F.; Zecchina, A.; Palomino, G.T; Areán, C.O. (1995). Fourier-transform infrared study of CO adsorbed at 77 K on H-Mordenite and alkali-metal-exchanged mordenites. *Langmuir*, *11*, 527-533.

28. López, R.; Gómez, R. (2012). Band-gap energy estimation from diffuse reflectance measurements on sol-gel and commercial TiO_2: A comparative study. *J. Sol-Gel Sci. Technol.*, *61*, 1-7.

29. Chen, Z.; Deutsch, T.G.; Dinh, H.N.; Domen, K.; Emery, K.; Forman, A.J.; Gaillard, N.; Garland, R.; Heske, C.; Jaramillo, T.F.; Kleiman-Shwarsctein, A.; Miller, E.; Takanabe, K.; Turner, J. (2013). UV-Vis Spectroscopy. Photoelectrochemical Water Splitting (pp. 49-62). *Springer.*

30. Mayerhöfer, T.G.; Pipa, A.V; Popp, J. (2019). Beer's Law-why integrated absorbance depends linearly on concentration. *ChemPhysChem*, *20*, 2748-2753.

31. Skoog, D.A.; Holler, F.J.; Nieman, T.A. (2000). Principios de Análisis Instrumental. *McGraw-Hill Interamericana de España.*

32. Lozano-Sánchez, J.; Borrás-Linares, I.; Sass-Kiss, A.; Segura-Carretero, A. (2018). Chromatographic Technique: High-Performance Liquid Chromatography (HPLC). Modern Techniques for Food Authentication (pp. 459-526). *Academic Press*.

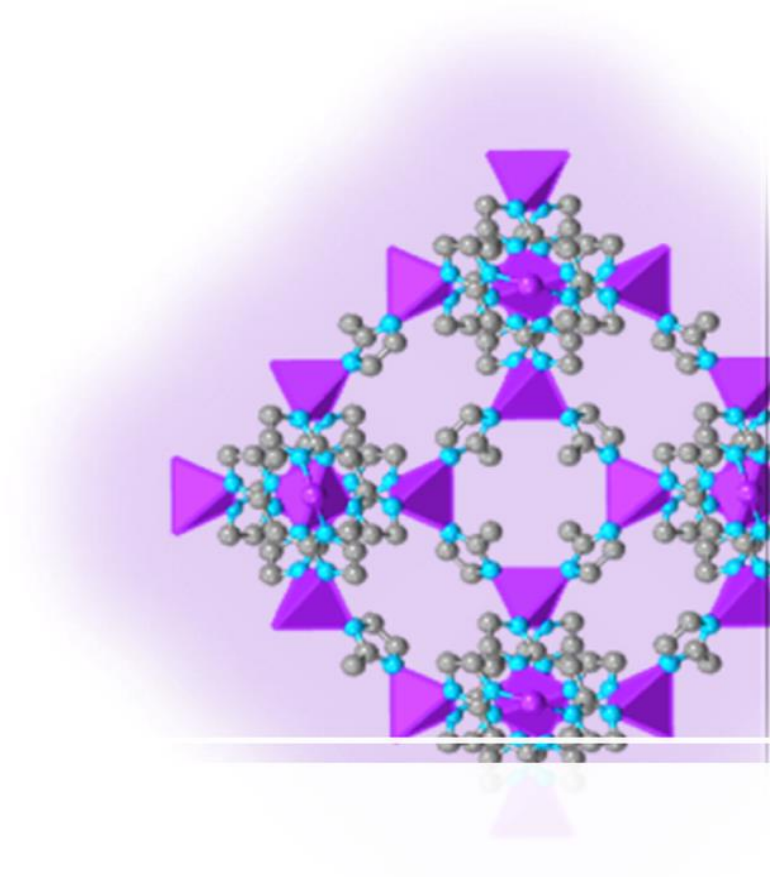

Chapter 4

Carbon composite membrane derived from MIL-125-NH_2 MOF for the enhanced extraction of emerging pollutants

Crespí Sánchez, N.; Guzmán-Mar, J.L.; Hinojosa-Reyes, L.; Turnes Palomino, G.; Palomino Cabello, C. (2019). *Chemosphere*, *231*, 510-517. DOI:10.1016/j.chemosphere.2019.05.173

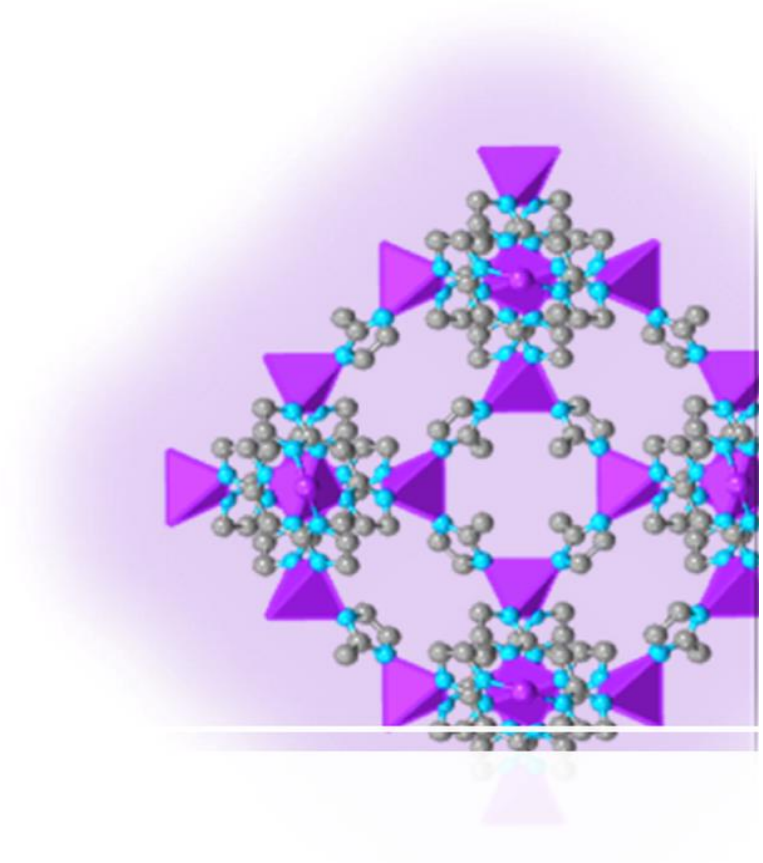

Chapter 5

NTU-9 derived TiO_2 coated stirrer as a highly efficient device for photocatalysis

Crespí Sánchez, N.; Turnes Palomino, G.; Palomino Cabello, C. (2019). *Mater. Sci. Eng. B*, *273*, 115424. DOI: 10.1016/j.mseb.2021.115424

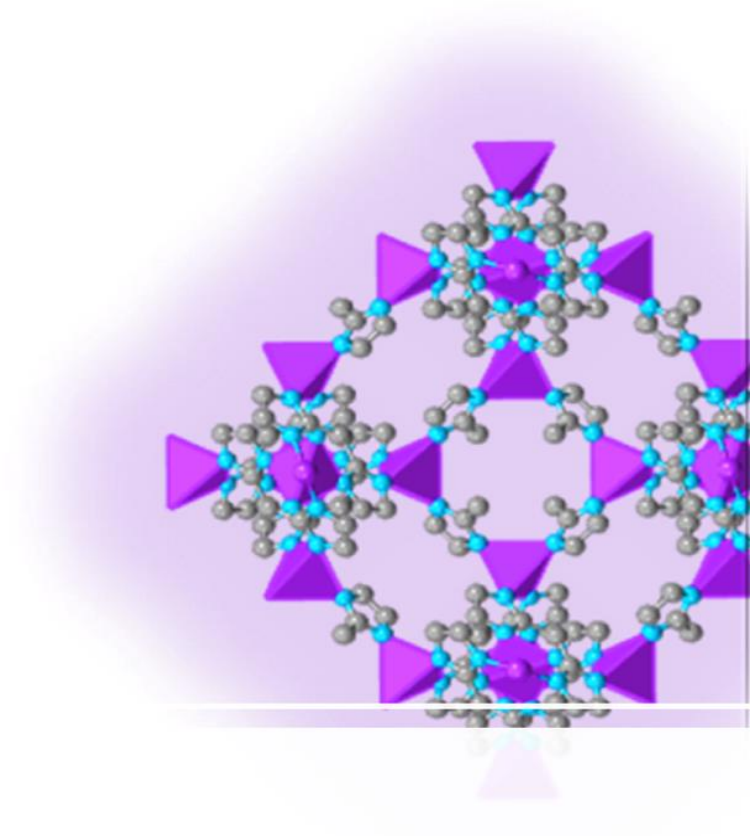

Chapter 6

Sulfonic-functionalized MIL-100-Fe MOF for the removal of diclofenac from water

Crespí Sánchez, N.; Turnes Palomino, G.; Palomino Cabello, C. (2023). *Microporous Mesoporous Mater.*, *348*, 112398. DOI: 10.1016/j.micromeso.2022.11239

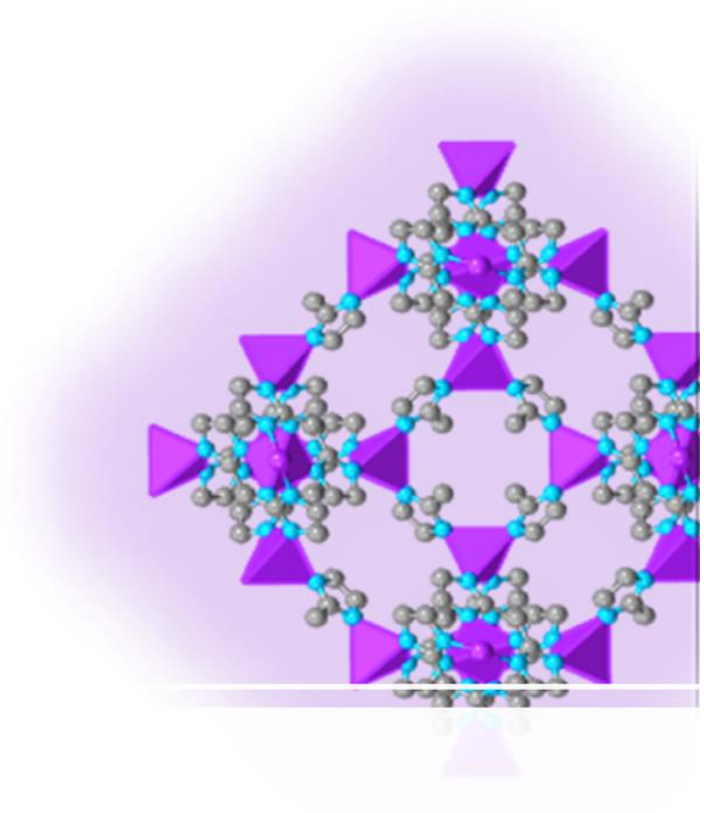

Chapter 7

General Conclusions

This chapter provides the conclusions of the present thesis.

Chapter 7: General conclusions

In this Doctoral Thesis, new porous solids based on MOFs and derived materials have been developed and tested in the adsorption and degradation of emerging and priority pollutants in aqueous samples.

Different types of MOFs have been synthesized by more environmentally friendly synthesis processes and, through their calcination in different atmospheres, MOF-derived materials have been prepared. In all cases, the obtained solids have been adequately characterised with different instrumental techniques. The prepared materials have demonstrated good performance in the removal of dyes, phenolic compounds and pharmaceuticals. Moreover, all of them have shown a great recyclability, with the additional advantage of being easily recoverable from the water medium due to their incorporation in different supports.

First, a porous carbon, derived from MIL-125-NH_2 MOF (C-MIL-125-NH_2) by a simple calcination process, has been prepared, characterized and tested as sorbent of emerging pollutants. After the calcination process, the C-MIL-125-NH_2 maintained the disk shape morphology of the precursor MOF, showed TiO_2 particles homogeneously distributed in the structure and micro and mesoporosity. The prepared carbon has demonstrated fast adsorption kinetics of BPA and 4-tBP, reaching equilibrium after 25 minutes for both pollutants. Moreover, by a simple method, using a nylon filter and PVDF as polymer binder, a mechanically stable hybrid membrane has been prepared and tested for the extraction and preconcentration of BPA and 4-tBP, obtaining enrichment factors of 109 and 46, respectively. The prepared hybrid membrane has also demonstrated its potential application for the simultaneous extraction and analysis of low levels of mixtures of environmental pollutants in real water samples, high ability to treat high volumes of polluted water and easy and excellent regenerability, making it a promising material for its use as adsorbent of different environmental pollutants in wastewater. Moreover, the developed methodology is easily extensible to obtain carbons from other MOFs, with a great potential in a large number of application fields, such as extraction or catalysis, among others.

Second, MOF-derived titanium oxide (TiO_2-NTU-9) has been obtained by calcination of NTU-9 MOF in air. The developed TiO_2 exhibited a narrow bandgap of 2.8 eV thanks to their mixed anatase/rutile phase structure and carbon doping. TiO_2-NTU-9 has been used as photocatalyst for the degradation of methylene blue dye under visible light, obtaining, in the

optimal experimental conditions, 100% of degradation after 2 h. In addition, the photocatalytic degradation efficiency of the prepared TiO_2 has been improved using hydrogen peroxide as oxidation agent, reaching, after 1 h, a percentage of degradation of 93%. A mechanically stable TiO_2-NTU-9 coated stirrer has been prepared by a simple and fast deposition method. The prepared hybrid stirrer has demonstrated high performance for MB removal (93% after 3 h of degradation), and easy recyclability, making it a promising material for water treatment.

Lastly, sulfonic-functionalized MIL-100-Fe (MIL-100-Fe-AMSA) with a surface area and pore volume of 845 $m^2 \cdot g^{-1}$ and 0.50 $cm^3 \cdot g^{-1}$, respectively, has been prepared by grafting aminomethane sulfonic acid to coordinatively unsaturated iron sites of MIL-100-Fe. MIL-100-Fe-AMSA has been effectively used as adsorbent of diclofenac, obtaining maximum extraction capacity of 476 $mg \cdot g^{-1}$, which is higher than that of the MIL-100-Fe, confirming the role of the sulfonic groups on the extraction process. In addition, the functionalized MOF has shown fast adsorption kinetics (>80% of extraction after only 4 min), high water stability and easy recyclability. The obtained MIL-100-Fe-AMSA was used for the preparation of a functional device (MIL-100-Fe-AMSA/3D column), which has exhibited high efficiency for the simultaneous extraction and preconcentration of DCF and ketoprofen under dynamic conditions, making it a promising device for the analysis of low levels of emerging pollutants from water.

To sum up, various advanced devices based on metal-organic frameworks and derived materials have been developed and applied to the extraction and degradation of various pollutants of environmental interest. The obtained results show that all the devices have great potential to monitor and treat polluted water.

Universitat
de les Illes Balears